INVESTIGATION OF CONVECTIVE HEAT TRANSFER COEFFICIENT FROM FINNED TUBES

A Thesis

Presented to

the Faculty of Graduate Studies and Research

The University of Manitoba

In Partial Fulfillment

of the Requirements for the Degree

Master of Science

---

by

George B. Babiy

March 1960

ACKNOWLEDGEMENTS

The author wishes to thank Professor R. E. Chant for his guidance and assistance in preparation of this thesis.

The writer is grateful to Mr. O. Tonn and Mr. J. Maguet for their advice and helpful suggestions in construction of the rig.

A special thanks is due to Mr. W. D. Gillies, who constructed part of the rig and patiently helped out in taking the readings.

The author also wishes to thank Mr. H. Weiss for his assistance in constructing the rig and for his help in making the drawings.

This thesis was sponsored by The National Research Council, whose interest is greatly appreciated. The funds were obtained in the form of a Summer Grant to the Department of Mechanical Engineering, The University of Manitoba.

ABSTRACT

INVESTIGATION OF CONVECTIVE HEAT TRANSFER COEFFICIENT FROM FINNED TUBE

by

George B. Babiy

Heat transfer coefficients were calculated for air "flowing over" a helically finned tube. The tube was heated internally with a 1-kilowatt calrod heater. The average and the local Stanton numbers were calculated and plotted against Reynolds numbers. Equation of the form $N_{Nu}/(N_{Pr})^{\frac{1}{3}} = 0.038\, N_{Re}^{0.8}$, based on the conventional equivalent diameter, was obtained. This equation can be used for calculating the average heat transfer coefficients for air "flowing over" a helically finned tube of a similar design to that used in this investigation. When the equivalent diameter based on the flow area between fins was used, the results for N_{Nu} were about 40 per cent lower than the results obtained using conventional equivalent diameter. The radial temperature gradients in the fin obtained from thermocouple measurements compared favourably with the calculated temperature gradients.

TABLE OF CONTENTS

PART PAGE

LIST OF TABLES

LIST OF FIGURES

NOMENCLATURE

LATIN LETTERS

A Heat flow area, ft^2

A_T Total heat flow area, ft^2

A_p Surface area of pipe, ft^2

A_f Surface area of fins, ft^2

C Constants

C_p Specific heat per unit mass, Btu/(lb)(°F)

D Diameter, ft

D_e Equivalent diameter ft; $D_e = \frac{4 \times \text{flow area}}{\text{wetted perimeter}}$

G Mass velocity, $lb/(hr)(ft^2)$

L Length, ft.

M Volume flow, ft^3/min; Velocity x Area

T Absolute temperature, °R

Q_t Total heat flow, Btu/hr

P Perimeter, ft

p Pressure, lb/in^2

Θ Temperature difference

J Mechanical equivalent of heat, 778.2 (ft)(lb)/Btu

b Width of the fin at the base, ft

d Diameter, ft

d_e Equivalent diameter based on the flow area between fins, ft; $d_e = \frac{4 \times \text{flow area between fins}}{\text{wetted perimeter}}$

d_a Density of air, lb/ft^3

d_w Density of water, lb/ft^3

f Friction factor

h Heat transfer coefficient in general, $Btu/(hr)(ft^2)(^oF)$

h_{fx} Heat transfer coefficient on the fin side of a pipe at station five, $Btu/(hr)(ft^2)(^oF)$

h_{fa} Average heat transfer coefficient on the fin side of a pipe, $Btu/(hr)(ft^2)(^oF)$

h'_{fx} Heat transfer coefficient on the fin side of a pipe at station five, but calculated from heat balance, $Btu/(hr)(ft^2)(^oF)$

h'_{fa} Average heat transfer coefficient on the fin side of a pipe, but calculated from heat balance, $Btu/(hr)(ft^2)(^oF)$

h_r Heat transfer coefficient for radiation, $Btu/(hr)(ft^2)(^oF)$

h_{va} Average height of water column, inches

K Thermal conductivity, $Btu/(hr)(ft)(^oF)$

l Length, ft

x, y, m, n Constants

X, Y, Z Coordinate axis, ft

y Distance from a plate, ft

t Temperature of fin or fluid in general, ^oF

t_g Temperature of air, ^oF

u Velocity in x-direction, ft/sec

u_∞ Velocity of the main stream ft/sec

v Velocity in y-direction, ft/sec

W Weight flow, lbs/hr

q Heat flow, Btu/hr or Btu/(hr)(ft^2)

GREEK LETTERS

α Thermal diffusivity, ft^2/hr

δ Boundary layer thickness, ft

ϵ Emissivity

μ Absolute viscosity lb/(ft)(hr)

ν Kinematic viscosity, ft^2/hr

ρ Density, lb/ft^3

σ Stefan-Boltzmann constant, 0.1714×10^{-8} Btu/(hr)(ft^2)($^oR^4$)

τ Shearing stress, lb/ft^2

ϕ Function

η_f Fin efficiency

η Boundary layer variable

θ' Dimensionless temperature ratio

MISCELLANEOUS

$\propto$ Proportional sign

∞ Infinity sign

$\sim$ Order of Magnitude sign

DIMENSIONLESS NUMBERS

Nusselt number, $N_{Nu} = \frac{h l}{K}$ or $\frac{h d}{K}$

Prandtl number, $N_{Pr} = \frac{\mu C_p}{K}$ or $\frac{\nu}{\alpha}$

Reynolds number, $N_{Re} = \frac{d G}{\mu}$, etc.

Stanton number, $N_{ST} = \frac{h}{C_p G}$

Other symbols as defined in the thesis.

INTRODUCTION

A survey of available literature indicated that not too much was published for the case of heat transfer to fluids flowing parallel to a tube axis, and still less for a flow parallel to a finned tube. The lack of information on this subject is due to the fact that heat transfer to a fluid flowing parallel to a tube axis is less efficient than heat transfer to a fluid flowing normal to a tube.

In recent years some industrial equipment was built, which required data on parallel flow heat transfer. Both the General Electric Company of England and the General Electric Company of Canada carried out some experiments on heat transfer to gases flowing parallel to finned tubes. These results were used in the design of uranium cans for nuclear reactors, but little of this was published.

E. Griffiths and J. H. Awbery[1*] described in their paper the investigations carried out on "heat transfer between the air and the outside of a pipe when set longitudinal to the air stream."

Heat transfer and pressure drop of liquids in double pipe finned tube exchangers were investigated by D. DeLorenzo and E. D. Anderson.[2] These experiments were

---

*Literature references are given in the References on page 62.

carried out on "standard size, longitudinally finned double pipe exchangers." The results were given in the form of curves, which could be readily used by a design engineer.

Heat transfer and pressure drop of gases in finned double pipe rigs were investigated by the General Electric Company of England.[3] A description of the rigs and some results in the form of curves were included in the above reference.

PART ONE

THEORETICAL CONSIDERATIONS

THREE DIFFERENT METHODS OF HEAT TRANSFER

Heat transfer is a science, which deals with the rates of exchange of heat between hot and cold bodies. There are three distinct modes of heat transfer: conduction, radiation, and convection. They have two phenomena in common: the existence of temperature differences and the transmission of heat from hot to cold body.

Conduction is the transfer of thermal energy from one molecule to another. The fundamental relation for steady state conduction was found by Biot and Fourier,

$$q_K = -K A \frac{dt}{dx}$$

Radiation is the transfer of heat by emission and absorption of thermal energy in form of rays. The rate at which energy is radiated from an area A, is

$$q_r = \epsilon \sigma A T^4$$

For a perfectly black body $\epsilon = 1$. The quantity σ is known as the "Stefan-Boltzmann" constant.

Convection is the transfer of heat by macroscopic motions. Newton developed an equation for this type of heat transfer: $q_C = h A \Delta t$

According to Newton, the latter type of heat transfer is the transfer of heat by macroscopic motion, (in transferring heat from a wall to a fluid, heat flow by conduction is present) and since most of the energy transfer takes place by physical displacement of fluids, we are justified to call this type of heat transfer as convection.

THE HEAT TRANSFER COEFFICIENT

In a paper on "Fluid Motion With Very Small Friction", in 1904, L. Prandtl proved that the flow about a solid body can be divided into two regions: a very thin layer in the neighborhood of the body called the boundary layer, where friction plays an essential part, and the remaining region outside this layer, where friction may be neglected.

This boundary layer develops because in real fluids the existence of shearing stresses causes the fluid to adhere to a solid wall. Thus the fluid, in this very thin region next to the wall, is substantially stationary with respect to the wall and heat transfer from the wall to this stationary fluid must be by conduction.

$$\left(\frac{\Delta t}{\Delta X}\right)_{\text{Stationary Layer}} = \frac{-q}{AK\,(\text{fluid})}$$

which gives as $\Delta x \longrightarrow 0$

$$\left(\frac{dt}{dx}\right)_{\text{Surface}} = \frac{-q}{AK(\text{fluid})}$$

As we move further away from the wall, we reach the fluid, which is in motion (active layer), and here the heat transfer is by convection.

For a system in which the wall temperature, t_s, the ambient temperature, t_∞, and the conductivity, k, of the fluid is constant, heat transmitted through the boundary layer is equal to the heat transmitted through the active layer, that is $q_c = q_k$.

But since $q_c = hA(t_s - t_\infty)$, $q_k = kA\left(\frac{dt}{dx}\right)_s$, and $\left(\frac{dt}{dx}\right)_s$ is the slope of the temperature profile in the fluid right at the wall,

$$h = \frac{-k\left(dt/dx\right)_s}{(t_s - t_\infty)}$$

This statement makes the heat transfer coefficient, h, a measure of the slope of the temperature distribution in the fluid right at the surface (see Figure 1).

The above equation gives a relationship between the convection and conduction, and also a physical interpretation of the heat transfer coefficient. If in the equation $q_c = hA(t_s - t_\infty)$, q_c is the total heat rate, which includes radiation, the coefficient, h, includes the radiation heat transfer also.

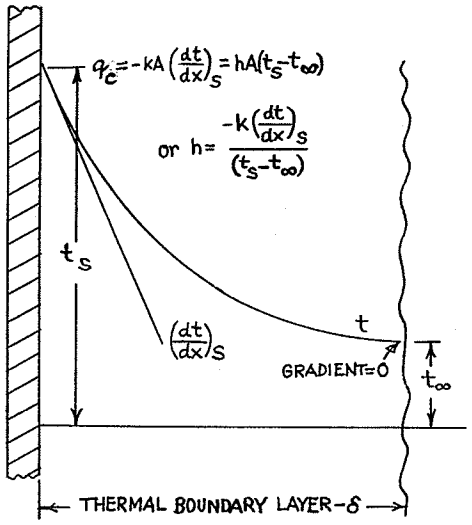

Figure 1. Physical interpretation of the heat transfer coefficient.

LAMINAR FLOW vs. TURBULENT FLOW

In laminar flow, the individual streamlines run side by side in orderly manner, while in turbulent flow, the streamlines move in an irregular motion. In 1883, O. Reynolds proved for the first time that these two different forms of flow exist. Heat exchange by convection is promoted by the fluctuating motions in turbulent flow. Thus, turbulence is of considerable interest when considering the heat transfer process. If we take, for example, a flat plate and investigate a flow parallel to the plate, we see that a boundary layer is formed close to the plate. Its thickness increases in the downstream direction (see Figure 2).

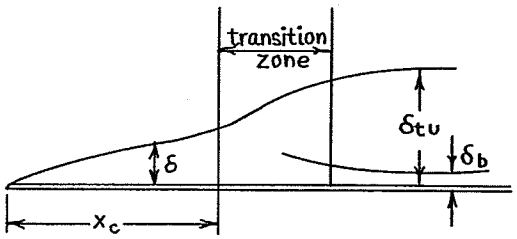

Figure 2. Laminar and turbulent boundary layers on a flat plate.

At a certain critical distance, x_c, from the leading edge, the flow within the boundary layer, which is at first laminar, changes into turbulent motion. The transition from the laminar to the turbulent boundary layer takes place in a transition zone. According to Prandtl, there is a laminar sublayer between the turbulent boundary layer and the wall. If tests are made with different fluids of various viscosities, it is found that the change from laminar to turbulent flow takes place at a definite value of a dimensionless term $\left(\frac{u_\infty x_c}{\nu}\right)$, called the Reynolds number.

LAMINAR FLOW-CONVECTIVE HEAT TRANSFER

a. General Considerations of Convective Heat Transfer

The study of convective heat transfer is generally considered as the exchange of energy between a surface and a fluid flowing over it. Since in this process, heat is conveyed mechanically, it is obvious that the transfer of energy depends upon the motion of the fluid and is governed

by the laws of fluid dynamics, as well as the laws of heat conduction.

The differential equations, which describe convective heat transfer belong to the most difficult class in theoretical physics. In this thesis, the study of convection deals with laminar flow of a fluid parallel to a flat plate, flow of a fluid in a tube and flow of a fluid in an annulus. Next comes the consideration of turbulent flow of a fluid parallel to a flat plate, flow of a fluid in a tube, flow of a fluid in an annulus, and flow of a fluid over extended surfaces.

b. Equation of Motion for Hydrodynamic Boundary Layer

To determine the differential equation of motion for two-dimensional viscous flow in a hydrodynamic boundary layer, we consider a 1 ft. wide section somewhere near the centre of a large plate, so that no side effects are present.[4]

We then proceed to make a momentum, energy, and mass balance for the parallelepiped-shaped volume element, $\Delta x \cdot \Delta y \cdot 1$, shown in Figure 3. The flow of fluids is governed by Newton's second law, namely, that the change in momentum per unit time is equal to the force acting in the x direction. The average mass flow into the left face and out the right is $\rho u \Delta y$. The change in momentum per unit time is, therefore

$$\rho u \Delta y \left(u + \frac{\partial u}{\partial x} \Delta x - u\right) = \rho u \frac{\partial u}{\partial x} \Delta x \Delta y \qquad \text{Eq. 1}$$

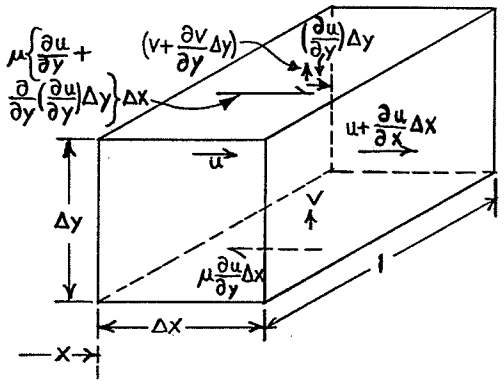

Figure 3. Velocity changes and viscous forces acting on a parallelepiped-shaped volume element.

The average mass flow rate into the bottom and out the top is $\rho v \Delta x$. Since the velocity, u, increases with y, the fluid flowing out through the top will have the component in x direction greater by an amount $\left(\frac{\partial u}{\partial y}\right)\Delta y$, over the fluid entering at the bottom. Therefore, the increment of momentum in the x direction of the fluid leaving the top, over the fluid entering at the bottom, is

$$\rho v \Delta x \frac{\partial u}{\partial y} \Delta y \qquad \text{Eq. 2}$$

The net force acting is simply the difference in the viscous drag on the upper and lower surfaces,

$$\mu \Delta x \left[\frac{\partial u}{\partial y} + \frac{\partial}{\partial y}\left(\frac{\partial u}{\partial y}\right)\Delta y - \frac{\partial u}{\partial y}\right] = \mu \frac{\partial^2 u}{\partial y^2} \Delta x \Delta y \qquad \text{Eq. 3}$$

Equating the sum of Equations 1 and 2 to Equation 3 gives

$$\rho u \frac{\partial u}{\partial x} + \rho v \frac{\partial u}{\partial y} = \mu \frac{\partial^2 u}{\partial y^2}$$

or

$$u \frac{\partial u}{\partial x} + v \frac{\partial u}{\partial y} = \nu \frac{\partial^2 u}{\partial y^2} \qquad \text{Eq. 4}$$

which is the equation of motion for the hydrodynamic boundary layer.

c. Energy Equation of the Thermal Boundary Layer

In Figure 4 are shown the quantities of energy entering and leaving a similar parallelepiped-shaped volume as in Figure 3. Since the rate of temperature change in x-direction is small, it can be neglected without introducing significant error.

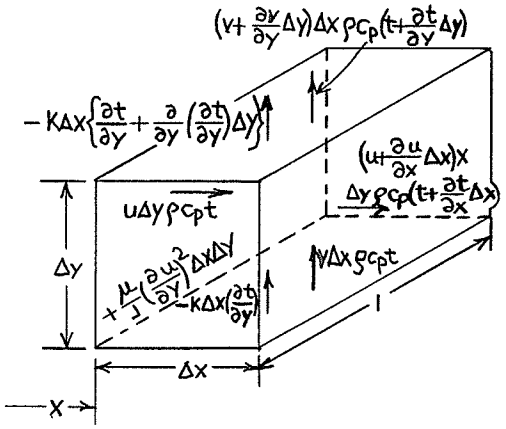

Figure 4. Energy quantities entering and leaving a parallelepiped-shaped volume element.

The net energy convected in the x direction is

$$u\,\Delta y\,\rho\,c_p\,t - \left(u+\frac{\partial u}{\partial x}\Delta x\right)\,\Delta y\,\rho\,c_p\left(t+\frac{\partial t}{\partial x}\Delta x\right)$$

which reduces to

$$-\rho c_p\left(u\frac{\partial t}{\partial x}+t\frac{\partial u}{\partial x}\right)\Delta x\,\Delta y \qquad \text{Eq. 5}$$

if the higher order term involving the product of $\left(\frac{\partial u}{\partial x}\right)\left(\frac{\partial t}{\partial x}\right)\Delta x^2\,\Delta y$ is neglected. A similar expression obtained for the energy balance in y direction is

$$-\rho c_p\left(v\frac{\partial t}{\partial y}+t\frac{\partial v}{\partial y}\right)\Delta x\,\Delta y \qquad \text{Eq. 6}$$

Since the temperature changes in x direction are negligible, conduction is considered in the y direction only. The net heat flow by conduction is then

$$-K\,\Delta x\frac{\partial t}{\partial y}-(-K\,\Delta x)\left\{\frac{\partial t}{\partial y}+\frac{\partial}{\partial y}\left(\frac{\partial t}{\partial y}\right)\Delta y\right\}=K\frac{\partial^2 t}{\partial y^2}\Delta x\,\Delta y \qquad \text{Eq. 7}$$

Finally, the heat generated by the fluid friction, which is the force times the distance divided by the mechanical equivalent of heat, must be considered. The average viscous force is $\mu\left(\frac{\partial u}{\partial y}\right)\Delta x$; the distance through which this force can be considered to act in unit time is determined by the relative movement of the fluid at the upper surface over that along the lower, and it is $\left(\frac{\partial u}{\partial y}\right)\Delta y$. The rate of energy added to the element is

$$\frac{\mu}{J}\left(\frac{\partial u}{\partial y}\right)^2\Delta x\,\Delta y \qquad \text{Eq. 8}$$

Considering that the temperature varies only with location and not time, the sum of various energy quantities entering the element volume is zero. Thus, adding Equations 5, 6, 7 and 8 yields

$$-\rho c_p\left\{u\frac{\partial t}{\partial x}+v\frac{\partial t}{\partial y}+t\left(\frac{\partial u}{\partial x}+\frac{\partial v}{\partial y}\right)\right\}\Delta x\,\Delta v+k\frac{\partial^2 t}{\partial y^2}\Delta x\,\Delta y+\frac{\mu}{J}\left(\frac{\partial u}{\partial y}\right)^2\Delta x\,\Delta y=0 \quad \text{Eq. 9}$$

The continuity equation for two-dimensional flow gives

$$\frac{\partial u}{\partial x}+\frac{\partial v}{\partial y}=0 \quad \text{Eq.10}$$

Using Equation 10, we can simplify Equation 9 to give

$$u\frac{\partial t}{\partial x}+v\frac{\partial t}{\partial y}=\frac{k}{\rho c_p}\frac{\partial^2 t}{\partial y^2}+\frac{\mu}{J\rho c_p}\left(\frac{\partial u}{\partial y}\right)^2 \quad \text{Eq. 11}$$

This equation is the differential energy equation for the flat plate.

d. Boundary Layer Thickness for a Flat Plate

At this time we want to find a solution for the velocity at any point (x, y) in the boundary layer for a flow over a plate as in Figure 5. The velocity distribution is

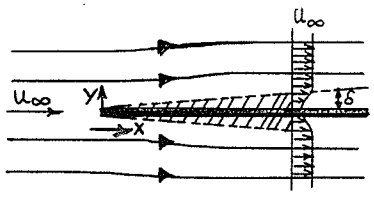

Figure 5. The boundary layer along a flat plate.

determined by solving first the hydrodynamic boundary layer equation (Equation 4) together with the continuity equation (Equation 10). This was the first example illustrating the application of Prandtl's theory, and was discussed by H. Blasius in his doctor's thesis at Goettingen.

Let the leading edge of the plate be at x = o, the plate being parallel to the x-axis and infinitely long downstream. We consider steady flow with a free stream velocity, u_∞, parallel to the x-axis.

The boundary conditions to be satisfied in the hydrodynamic boundary layer equation (Equation 4) are:

$$u = 0 \quad \text{and} \quad v = 0 \quad \text{at} \quad y = 0$$

$$u = u_\infty \quad \text{at} \quad y = \infty$$

The reasoning to the solution of Equation 4 started with the order of magnitude analysis of the boundary layer thickness, δ.

The terms on the left hand side of Equation 4 represent the inertia forces and are balanced by the viscous forces given by the term on the right hand side. Since $u \gg v$,

$\rho u \frac{\partial u}{\partial x} \propto \mu \frac{\partial^2 u}{\partial y^2}$ may be considered as first approximation of Equation 4. Also, since u is of the same order of magnitude as u_∞, $\frac{\partial u}{\partial x} \sim \frac{u_\infty}{x}$; therefore $u \frac{\partial u}{\partial x} \sim \frac{u^2_\infty}{x}$, and

$\frac{\partial u}{\partial y} \sim \frac{u_\infty}{\delta}$, so that the viscous force $\mu \frac{\partial^2 u}{\partial y^2}$ is of the order $\mu \frac{u_\infty}{\delta^2}$. Since also $\rho u \frac{\partial u}{\partial x} \sim \mu \frac{\partial^2 u}{\partial y^2}$ we get

$$\rho \frac{u_\infty^2}{x} \sim \mu \frac{u_\infty}{\delta^2} \qquad \text{Eq. 12}$$

or solving for the boundary layer thickness δ ,

$$\delta \sim \sqrt{\frac{\mu x}{\rho u_\infty}} \sim \sqrt{\frac{\nu x}{u_\infty}} \qquad \text{Eq. 13}$$

It is reasonable to suppose that the velocity profiles at various distances from the leading edge are similar to each other. Hence, the velocity profile at any location x in the boundary layer can be written as $\frac{u}{u_\infty} = F\left(\frac{y}{\delta}\right)$ and it must change along the plate according to some scale factor involving only x.

We now introduce a new variable $\eta = \frac{y}{\delta}$, which is a function of x and y and a function f which is a function of η alone. The variable η is defined by

$$\eta = y\sqrt{\frac{u_\infty}{\nu x}} \qquad \text{Eq. 14}$$

By introducing

$$u = \frac{\partial \psi}{\partial y} \qquad \text{Eq. 15}$$

as the definition of a stream line function, we get

$$u = \frac{\partial \psi}{\partial \eta} \times \frac{\partial \eta}{\partial y} = u_\infty \frac{df}{d\eta} \quad * \qquad \text{Eq. 16}$$

Similarly, the transverse velocity component is

$$v = -\frac{\partial \psi}{\partial x} = \frac{1}{2}\sqrt{\frac{\nu u_\infty}{x}}\left(\eta \frac{df}{d\eta} - f\right) \qquad \text{Eq. 17}$$

Now substituting from Equations 16 and 17 into Equation 4, we get

$$\frac{-u_\infty^2}{2x}\eta \frac{df}{d\eta}\frac{d^2f}{d\eta^2} + \frac{u_\infty^2}{2x}\left(\eta \frac{df}{d\eta} - f\right)\frac{d^2f}{d\eta^2} = \nu \frac{u_\infty^2}{x\nu}\frac{d^3f}{d\eta^3}$$

After simplification, the following ordinary differential equation is obtained

$$f\frac{d^2f}{d\eta^2} + 2\frac{d^3f}{d\eta^3} = 0 \qquad \text{Eq. 18}$$

The boundary conditions are

$$\text{at } \eta = 0 : \; f = 0 \text{ and } \frac{df}{d\eta} = 0 \; ; \; \text{at } \eta = \infty \; : \frac{df}{d\eta} = 1$$

Thus, the partial differential Equation 4 has been transformed into an ordinary differential equation of the third order.

The evaluation of the solution of the differential Equation 4 is not very simple, and the general solution

---

*Derivation of Eq. 16 is shown in Appendix A.

cannot be obtained. H. Blasius obtained the solution in the form of a series expansion in the year 1908.

It is impossible to indicate a boundary layer thickness in a definite way, because the viscosity in the boundary layer decreases asymptotically outwards. If we define the boundary layer thickness as that distance for which $u = 0.99\, u_\infty$, then $\eta \sim 5.00$, as seen from the solution of the boundary layer Equation 18 by L. Howarth.[5] Hence, the boundary layer thickness, as defined here, becomes

$$\delta \approx 5.0 \sqrt{\frac{\nu x}{u_\infty}} \qquad \text{Eq. 19}$$

Presently, however, a value called the "displacement thickness δ^*" is almost generally accepted. Mathematically, it is obtained from the equation

$$\delta^* = \int_{y=0}^{\infty} \left(1 - \frac{u}{u_\infty}\right) dy \qquad \text{Eq. 20}$$

The displacement thickness is that distance by which the external potential field of flow is displaced outward as a consequence of the decrease in velocity in the boundary layer. Blasius found that

$$\delta^* = 1.73 \sqrt{\frac{\nu x}{u_\infty}} = \frac{1.73x}{\sqrt{N_{Re}}} \qquad \text{Eq. 21}$$

where x is the distance from the leading edge of the plate.

As it was stated, the computation of the boundary

layer Equation 18 is difficult and lengthy. However, an approximate method for the solution of the boundary layer thickness, which originated by T. von Kárman,[6] will be used.

This method starts from the law of momentum as described on page 6, namely

Momentum = mass.velocity

The above law may now be applied to a two-dimensional flow along a flat plate (Figure 6) for the x direction. Use

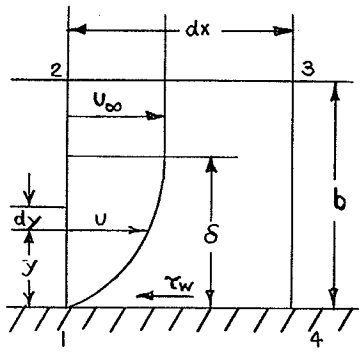

Figure 6. Calculation of the boundary layer thickness.

is also made of the following: the velocities have essentially a direction parallel to the wall, and only small velocities normal to the wall exist. Consider a surface built by four planes 1-2, 2-3, 3-4 and the wall 4-1, spaced apart from each other as in Figure 6. The distance b may be greater than the boundary layer thickness, δ . The velocity profile in the plane 1-2 has the sketched shape. At a distance y from the wall, the velocity is u . The outside velocity, u_∞, is reached within the length b , at the distance δ from the wall. Now consider a 1 ft. wide surface.

Through a differential strip dy at a distance y, the mass flow per unit time is $\rho u dy$. Its momentum is equal to the mass flow multiplied by the velocity u. The momentum flow through the whole plane 1-2 is

$$\rho \int_0^b u^2 \, dy$$

In the x direction this momentum flow changes by

$$\rho \frac{d}{dx} \left(\int_0^b u^2 dy \right) dx = \rho \, dx \frac{d}{dx} \int_0^b u^2 \, dy$$

There is no flow through the wall 1-4. The flow through the plane 2-3 may be calculated in the following way. The mass flow through plane 1-2 per unit time is $\rho \int_0^b u dy$. Moving through the distance dx, this flow changes by $\rho dx \frac{d}{dx} \int_0^b u dy$. This is the difference between the flow through the planes 3-4 and 1-2, and it must have entered the cube through plane 2-3. The velocity component in the x direction in this plane is u_∞. Therefore, the momentum flow in x direction through plane 2-3 is

$$\rho u_\infty dx \frac{d}{dx} \int_0^b u \, dy$$

The whole increase in momentum within the cube is, therefore,

$$-\rho u_\infty dx \frac{d}{dx} \int_0^b u \, dy + \rho \, dx \frac{d}{dx} \int_0^b u^2 dy$$

$$= -\rho dx \frac{d}{dx} \int_0^b (u_\infty - u) \, u dy + \rho \, dx \frac{du_\infty}{dx} \int_0^b u \, dy$$

Since the velocity potential flow is constant, $\frac{dP}{dx} \equiv 0$, the only external force acting on the surface of the parallelepiped-shaped volume in the x direction is the shearing stress, τ_w, along the wall. Equating this force with the increase in momentum,

$$\rho \frac{d}{dx}\int_0^b (u_\infty - u)\, u\, dy - \rho \frac{du_\infty}{dx}\int_0^b u\, dy = \tau_w \qquad \text{Eq. 22}$$

Since the velocity, u_∞, outside the boundary layer is constant along the plate, Equation 22 simplifies to

$$\rho \frac{d}{dx}\int_0^b (u_\infty - u)\, u\, dy = \tau_w \qquad \text{Eq. 23}$$

Equation 23 can be solved (according to von Kármán's suggestion) when the approximate shape of the velocity profile is known.

The velocity profile in a laminar boundary layer was found by measurements to be similar to a parabola. It is, however, more suitable to use a cubic parabola* $u = by + dy^3$ Therefore for

$$y = 0 \quad : \quad u = 0$$

and for

$$y = \delta \quad : \quad u = u_\infty \quad \text{and} \quad \frac{du}{dy} = 0$$

This gives $b = \frac{3}{2}\,\frac{u_\infty}{\delta} \qquad d = -\frac{1}{2}\,\frac{u_\infty}{\delta^3}$

---

* Reason given in Appendix A.

and

$$\frac{u}{u_\infty} = \frac{3}{2}\,\frac{y}{\delta} - \frac{1}{2}\left(\frac{y}{\delta}\right)^3 \qquad \text{Eq. 24}$$

With this equality the integral in Equation 23 becomes*

$$\int_0^b (u_\infty - u)\,u\,dy = u_\infty^2 \int_0^\delta \left\{\frac{3}{2}\,\frac{y}{\delta} - \frac{1}{2}\left(\frac{y}{\delta}\right)^3\right\}\left\{1 - \frac{3}{2}\,\frac{y}{\delta} + \frac{1}{2}\left(\frac{y}{\delta}\right)^3\right\} dy$$

$$= \frac{39}{280}\,u_\infty^2\,\delta \qquad \text{Eq. 25}$$

From Equation 24,

$$u = u_\infty\left\{\frac{3}{2}\,\frac{y}{\delta} - \frac{1}{2}\left(\frac{y}{\delta}\right)^3\right\}$$

and

$$\left(\frac{\partial u}{\partial y}\right) = u_\infty\left\{\frac{3}{2}\,\frac{1}{\delta} - \frac{3}{2\delta}\left(\frac{y}{\delta}\right)^2\right\}$$

thus

$$\left(\frac{\partial u}{\partial y}\right)_{y=0} = \frac{3}{2}\,\frac{u_\infty}{\delta}$$

Therefore, the shearing stress $\tau_w = \mu\frac{\partial u}{\partial y} = \frac{3}{2}\,\mu\,\frac{u_\infty}{\delta}$

Introducing this expression and the value of Equation 25 in Equation 23, the following equation results:

$$\frac{39}{280}\,\rho u_\infty^2\,\frac{d\delta}{dx} = \frac{3}{2}\,\mu\,\frac{u_\infty}{\delta}$$

---

*Integration accomplished in Appendix A.

and by separating the variables,

$$\delta\, d\delta = \frac{140}{13}\,\frac{\nu}{u_\infty}\,dx$$

Integrating the above gives

$$\delta = 4.64\sqrt{\frac{\nu x}{u_\infty}} + C \qquad \text{Eq. 26}$$

When $x = 0$ $\delta = 0$, and $C = 0$

Therefore, Equation 26 becomes

$$\frac{\delta}{x} = \frac{4.64}{\sqrt{N_{Re}}} \qquad \text{Eq. 27}$$

The boundary layer thickness δ is the distance from the wall, where the velocity, as approximated by Equation 24, reaches the value of the outside flow velocity. When so defined, the boundary layer thickness is somewhat arbitrary, because the exact calculation of laminar boundary layers gives the velocity profile, which reaches the outside velocity asymptotically. Other definitions, as given on page 14, are also used.

e. The Prandtl Number

When the last term on the right hand side of Equation 11 is neglected, and $\frac{K}{WC_p}$ is equated to α, it may be observed that when $\alpha = \nu$, Equation 11 is identical to Equation 4, when temperature in Equation 11 is replaced by velocity u.

Therefore, whenever $\alpha = \nu$ the temperature distribution is identical to the velocity distribution at any point (x,y) from the leading edge of the plate, and when the plate has a temperature t_s, the

temperature distribution, according to Equation 16, is:

$$\frac{t - t_s}{t_\infty - t_s} = \frac{u}{u_\infty} = \frac{df}{d\eta} \qquad \text{Eq. 28}$$

Equation 28 is of considerable practical importance because for all gasses, α is approximately equal to ν . It also suggests that the more the ratio ν/α differs from unity, the greater will be the difference between the temperature and velocity profiles. The ratio of ν to α is defined as the Prandtl number

$$N_{Pr} = \frac{\nu}{\alpha} = \frac{\mu c_p}{k} \qquad \text{Eq. 29}$$

f. Temperature Distribution in the Boundary Layer

In solving Equation 11 for the temperature distribution in the boundary layer, we assume that

$$\theta'(\eta) = \frac{t(\eta) - t_s}{t_\infty - t_s} \qquad \text{Eq. 30}$$

and also that the solution of the hydrodynamic boundary layer is available.

H. Blasius introduced new variables, (similarly as in solving Equation 4), which lead to the following ordinary differential equation:

$$\frac{d^2\theta'}{d\eta^2} + \frac{1}{2} N_{Pr} f \frac{d\theta'}{d\eta} = 0 \qquad \text{Eq. 31}$$

with $\theta' = 0$ at $\eta = 0$ and $\theta' = 1$ at $\eta = \infty$. The solution of

Equation 31 was given by Pohlhausen.[4,5] He found that

$$\frac{d\,\theta'(o)}{d\eta} = 0.332\ N_{Pr}^{\frac{1}{3}} \qquad \text{Eq. 32.}$$

g. The Local Heat Transfer Coefficient and the Local Nusselt Number

The rate of heat flux per unit time at any location x along a plate is by definition

$$q_{(x)} = -k\left(\frac{\partial t}{\partial y}\right)_{y=0} = h_x(t_s - t_\infty) \qquad \text{Eq. 33}$$

where $\partial t/\partial y$ is the slope of the temperature distribution in the fluid at $y = 0$ and location x along the plate, K is the fluid thermal conductivity and h_x is the local heat transfer coefficient.

Solving Equation 33 for h_x, gives

$$h_x = \frac{-k\left(\frac{\partial t}{\partial y}\right)_{y=0}}{(t_s - t_\infty)} \qquad \text{Eq. 34}$$

From the definition of $\theta'(\eta)$, as defined in Equation 30 we get

$$\left(\frac{\partial t}{\partial y}\right)_{y=0} = (t_\infty - t_s)\left(\frac{\partial \theta'}{\partial y}\right)_{y=0} = (t_\infty - t_s)\left\{\frac{\partial \theta'}{\partial \eta} \times \frac{\partial \eta}{\partial y}\right\}_{y=0} \qquad \text{Eq. 35}$$

and from Equations 32 and 16

$$\frac{\partial t}{\partial y} = 0.332\ N_{Pr}^{\frac{1}{3}}\ \sqrt{\frac{u_\infty}{\nu x}}\ (t_\infty - t_s) \qquad \text{Eq. 36}$$

Substituting Equation 36 into Equation 34 yields

$$h_x = 0.332\ k\ N_{Pr}^{\frac{1}{3}} \sqrt{\frac{u_\infty}{\nu x}} \qquad \text{Eq. 37}$$

or multiplying each side of Equation 37 by $\frac{x}{k}$ we get

$$\frac{h_x x}{k} = 0.332\ N_{Pr}^{\frac{1}{3}}\ \ N_{Re_x}^{\frac{1}{2}} \qquad \text{Eq. 37a}$$

Thus, the local heat transfer coefficient varies along the plate inversely as $x^{\frac{1}{2}}$, as shown in Figure 7.

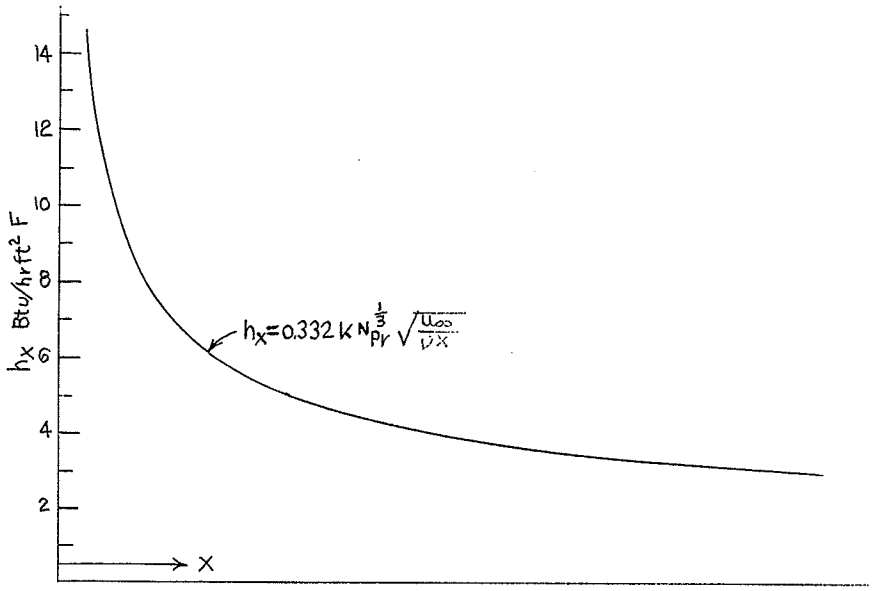

Figure 7. Variation of local heat transfer coefficient along a flat plate.

h. The Average Heat Transfer Coefficient and the Average Nusselt Number

The total heat transferred from a plate 1 ft. wide can be obtained by integrating the local rate of heat transfer over the entire length, l . The local rate of heat transfer

$$q_x = -k\left(\frac{\partial t}{\partial y}\right)_{y=0}$$

Therefore the total heat transferred from the above plate is

$$q_a = -k\int_0^l \left(\frac{\partial t}{\partial y}\right)_{y=0} dx = \int_0^l h_x \left(t_s - t_\infty\right) dx \qquad \text{Eq. 38}$$

Substituting the value for h_x from Equation 37 we obtain:

$$q_a = 0.332\, k\, N_{Pr}^{\frac{1}{3}} \left(t_s - t_\infty\right) \int_0^l \sqrt{\frac{u_\infty}{\nu x}}\, dx$$

$$= 0.332\, k\, N_{Pr}^{\frac{1}{3}} \left(t_s - t_\infty\right) \int_0^l \sqrt{\frac{u_\infty}{\nu}}\, x^{-\frac{1}{2}}\, dx$$

$$= 0.664\, k\, N_{Pr}^{\frac{1}{3}} \sqrt{\frac{u_\infty l}{\nu}} \left(t_s - t_\infty\right) \qquad \text{Eq. 39}$$

Defining the average heat transfer coefficient as

$$h_a = \frac{q_a}{l\left(t_s - t_\infty\right)} \qquad \text{Eq. 40}$$

and equating Equations 39 and 40 the following expression for h_a is obtained:

$$h = 0.664\, k\, N_{Pr}^{\frac{1}{3}} \sqrt{\frac{u_\infty}{\nu l}} \qquad \text{Eq. 41}$$

or multiplying each side of Equation 41 by l/k we get

$$\frac{h_a l}{k} = 0.664\, N_{Pr}^{\frac{1}{3}}\, N_{Re}^{\frac{1}{2}} \qquad \text{Eq. 42}$$

It can be seen from Equations 37 and 41 that the average heat transfer coefficient, h_a, over a length, L, of the plate is twice the local heat transfer coefficient, h_x, at $x = L$.

The dimensionless ratio on the left hand side of Equation 37a is called the local Nusselt number, N_{Nux}, and the term on the left hand side of Equation 42, the average Nusselt number, $\overline{N_{Nu}}$.

A useful relation between the local N_{Nux} and the corresponding friction factor, f, is obtained by dividing Equation 37a by $N_{Rex} N_{Pr}^{\frac{1}{3}}$, or

$$\left(\frac{N_{Nux}}{N_{Rex} N_{Pr}}\right) N_{Pr}^{\frac{2}{3}} = \frac{0.322}{N_{Rex}^{\frac{1}{2}}} = \frac{f}{2} = j \qquad \text{Eq. 43}$$

The dimensionless ratio $N_{Nux}/N_{Rex} N_{Pr}$ is known as the Stanton number, N_{Stx}, and was proposed by Colburn[4] on the basis of experimental data.

i. Heat Transfer by Forced Convection in Laminar Flow in Tubes.

The heat transfer coefficients available through natural convection mechanisms are very small. Forced convection, on the other hand, may offer coefficients hundreds of times higher than those available through natural convection.

For engineering applications, it is most convenient to present results of analytical and experimental investigations in terms of the Nusselt number, defined similarly as in Equation 42, except that a diameter instead of a length is used for flow in tubes.

Thus $N_{Nu\,x} = \frac{h_x d}{k}$.

The convective coefficient, h_x, varies along the tube. For this reason, a mean Nusselt number, $\overline{N_{Nu}}$, is needed. The mean Nusselt number is obtained from the average convective coefficient, h_a.

Since $h_a = \frac{1}{l}\int_0^l h_x \, dx$, where l is the pipe length, and the subscript x refers to local conditions at x, the mean Nusselt number $\overline{N_{Nu}} = h_a \frac{d}{k}$

A detailed mathematical solution for forced convection in laminar flow in tubes is very complicated. References such as 7 and 8 develop equations which are presented below. Reference 7 gives also a set of curves for N_{Nu_x} against $N_{Re} N_{Pr} \frac{d}{x}$. These curves are the results of work of various investigators. For very long tubes, N_{Nu_x} has a value of 3.65, when the tube temperature is uniform, and N_{Nu_x} is 4.36, when the heat rate is uniform.

For practical calculations, the following empirical formula, for fully developed flow, is given by Kays: [7]

$$\overline{N_{Nu}} = \frac{h_a d}{K} = 3.65 + \frac{0.0668 (d/l) N_{Re} \quad N_{Pr}}{1 + 0.04 \left\{ (d/l) \; N_{Re} \quad N_{Pr} \right\}^{\frac{2}{3}}} \qquad \text{Eq. 44}$$

TURBULENT FLOW-CONVECTIVE HEAT TRANSFER

Reynolds observed that the type of flow a liquid assumes flowing in a tube, is influenced by the velocity, the density, and the viscosity of the liquid, as well as the diameter of the tube. He found that turbulent flow exists when the Reynolds number, $N_{Re} = \frac{GD}{\mu}$, exceeds 2,100. Fully developed turbulent flow in a fluid stream is generally considered to be bounded by a lower Reynolds number of 10,000.[15]

Although some progress has been made in the analysis of heat transfer in turbulent flow, most calculations at the present time are based on semi-empirical equations, correlated by experimental data. Almost all correlations in present use have been arrived at through dimensional analysis.

a. Use of Dimensional Analysis in Developing Heat Transfer Equations for Turbulent Flow.

One of the important mathematical proofs of dimensional analysis is attributed to Buckingham, [16] who deduced, that if there are n physical variables in a particular problem, and m fundamental units (such as length, mass, time, etc.), then the number of dimensionless groups in the physical equation equals the number of variables minus the number of fundamental units. Dimensional constants are also

included as variables. Designating dimensionless groups by the letters π_1, π_2, π_3, the complete physical statement of a phenomenon can be expressed by

$$\phi\left(\pi_1, \pi_2, \pi_3 \cdots\right) = 0 \qquad \text{Eq. 45}$$

The most serious limitation of dimensional analysis is that it gives no information about the nature of a phenomenon. In fact, to apply dimensional analysis, it is necessary to know beforehand what variables influence the phenomenon. Thus, in order to develop a mathematical expression for the surface coefficient of turbulent forced convection, it is necessary first to establish which variables effect the problem. The convective coefficient, h_a, for a fluid flowing at constant mass rate in a pipe of uniform diameter, has been found to be influenced by the velocity, v, the density, ρ, specific heat, c_p, thermal conductivity, k, viscosity, μ, as well as the inside diameter of the pipe, D.

Thus, using $ML\theta T$ system, we can express the seven physical quantities in terms of four fundamental dimensions, and obtain three dimensionless groups, or three π terms in the result. Solving for each fundamental dimension separately, we obtain the following three dimensionless groups:

$$\pi_1 = \frac{h_a D}{k}$$

which is recognized as the Nusselt number, $\overline{N_{Nu}}$;

$$\pi_2 = \frac{V D \rho}{\mu} = \frac{D G}{\mu}$$

which is recognized as the Reynolds number, N_{Re} ;

and $$\pi_3 = \frac{C_p \mu}{k}$$

which is recognized as the Prandtl number, N_{Pr} .

The final expression, for the surface coefficient of turbulent forced convection, according to Equation 45 is

$$\phi\left(\overline{N_{Nu}}, N_{Re}, N_{Pr}\right) = 0$$

or

$$\frac{hD}{k} = f_1\left(\frac{DG}{\mu}\right) f_2\left(\frac{C_p \mu}{k}\right) = C\left(\frac{DG}{\mu}\right)^x \left(\frac{C_p \mu}{k}\right)^y \qquad \text{Eq. 46}$$

where the constant C, and the exponents x and y must be evaluated from the experimental data.

b. Turbulent Flow - Convective Heat Transfer Parallel to Plane Surfaces.

Jakob[8] developed a formula for a forced heat convection in turbulent flow parallel to a plane plate at uniform temperature. He states that "it is supposed that the plate is so thin that the leading edge does not affect the arriving stream." Neglecting the heating effect of friction and assuming uniform pressure, he arrives at the following formula

$$\frac{hL}{k} = 0.0366 \left(\frac{V_o L}{\nu}\right)^{0.8} \frac{\nu}{\alpha} \qquad \text{Eq. 47}$$

where the surface is of unit width, and the length in the

direction of flow is L.

Experiments[9] on the flow of air, as a cooling medium flowing parallel to smooth surfaces, indicate that the surface coefficient for turbulent flow may be expressed by the equation

$$h = 0.55\frac{k}{L}\left(\frac{LG}{\mu}\right)^{0.75} \qquad \text{Eq. 48}$$

This equation was developed from dimensional analysis and although based on tests with atmospheric air only, and with the length of the surface, L, about 1 ft., is applicable for calculation of h_a for plates longer than 2 ft. In this case, L equal to 2 ft. is to be used, because beyond the length of 2 ft., turbulence is probably fully developed. Equation 48 can be used for any gas over a considerable range of variation in physical properties.

W. McAdams[10] gives two equations and a set of curves to be used for a gas flowing parallel to a single plate.

c. Turbulent Flow - Convective Heat Transfer in Tubes

Efforts to correlate the data of various experiments, performed on fluids in turbulent flow in tubes by various investigators, have resulted in slightly different values for the constant and exponents in Equation 46.

Possibly the best known and most widely used form of Equation 46 is the following given by McAdams:[10]

$$\frac{hD}{k_B} = 0.023\left(\frac{DG}{\mu_B}\right)^{0.8}\left(\frac{C_p\mu}{k}\right)^{y}_{B} \qquad \text{Eq. 49}$$

where the subscript B indicates that the physical properties are to be evaluated at the average bulk temperature of the fluid. Equation 49 is ordinarily used for fluids having viscosities not more than twice that of water. The exponent y in Equation 49 is 0.3 for cooling and 0.4 for heating.

For liquids of high viscosity, and Reynolds numbers exceeding 10,000, instead of following the old procedure of using Equation 49, it is more logical to use the Colburn[11] equation

$$\frac{hD}{k_f} = 0.023\left(\frac{DG}{\mu_f}\right)^{0.8}\left(\frac{C_p\mu_f}{k}\right)^{\frac{1}{3}} \qquad \text{Eq. 50}$$

where the subscript f indicates that the physical properties are to be evaluated at the average film temperature. All other physical properties are to be evaluated at the average bulk temperature.

Examinations of the values of C_p, k, μ, and p for various fluids at different temperatures show, that in the case of viscous liquids, the property that is most affected by change in temperature is the viscosity, μ. On the basis of this observation Sieder and Tate[12] made a correlation of both heating and cooling of viscous liquids in turbulent flow and

arrived at the following equation

$$\frac{hD}{k} = 0.027\left(\frac{DG}{\mu}\right)^{0.8}\left(\frac{C\mu}{k}\right)^{\frac{1}{3}}\left(\frac{\mu}{\mu_w}\right)^{0.14} \qquad \text{Eq. 51}$$

where all physical properties are evaluated at the average bulk temperature, except μ_w, which is evaluated at the wall temperature.

Equations 49, 50 and 51 are recommended to be used for turbulent flow in pipes and tubes of at least 40 diameters in length. For turbulent flow in short pipes and tubes, apply correction factors.[9]

For turbulent flow in ducts, Equations 49, 50 and 51 can be used, except that an equivalent diameter, D_e, has to be substituted for D.

d. Turbulent Flow - Convective Heat Transfer Outside and Parallel to Tubes.

When a fluid flows in a conduit having other than a circular cross section, such as an annulus, it is convenient to express the heat transfer coefficient by the same types of equations and curves as used for pipes and tubes. Test data for the case of gases flowing in an annulus are in rough agreement with the equations for gases inside pipes or tubes when D_e is used.[13]

Donohue[14] states that for turbulent flow outside tubes, the following equation should be used

$$\frac{hD}{k} = C \left(\frac{DG}{\mu}\right)^{0.6} \left(\frac{C_p \mu}{k}\right)^{0.33} \left(\frac{\mu}{\mu_w}\right)^{0.14} \qquad \text{Eq. 52}$$

where C = numerical constant varying with each unit

D = outside tube diameter

Further, Donohue states that in seeking an explanation for the variation of the value of C in Equation 52 where the only pertinent variable was the arrangement of the tubes (in the tests performed), it was found that

$$C = 0.128 \left(D_e'\right)^{0.6}$$

where D_e' = equivalent diameter, inches.

Therefore, rewriting Equation 52, we get

$$\frac{hD}{k} = 0.128 \left(D_e'\right)^{0.6} \left(\frac{DG}{\mu}\right)^{0.6} \left(\frac{C_p \mu}{k}\right)^{0.33} \left(\frac{\mu}{\mu_w}\right)^{0.14} \qquad \text{Eq. 53}$$

TURBULENT FLOW OVER EXTENDED SURFACES

When additional metal pieces are attached to ordinary heat transfer surfaces, such as pipes or tubes, they extend the surface available for heat transfer, and thus, increase the heat transfer coefficient. In particular, fins are used with fluids having high thermal resistance, as for example air.

For fluids flowing over extended surfaces, the flow becomes so complicated "that it may never be possible accurately to predict their performance through formal

mathematics."[15] The major difference between these surfaces, and the simple tubes and flat plates, is in the lack of any transition region in almost all the extended surfaces.

For a given mass flow of air, it was found, that the highest coefficients of heat transfer were obtained for a flow normal to transverse fins, intermediate coefficients for a flow parallel to discontinuous strips and the lowest coefficients for a flow parallel to continuous or longitudinal fins.

For this reason, there is but little data published for flow of air or any other fluid parallel to longitudinal or helical fins.

a. Radial Temperature Distribution in Fins

The theory for convective heat transfer from fins was first developed from the theory of heat flow from a rod, connected at its base to a heated wall, and cooled on its surface by a fluid flowing over it.

1. Temperature Distribution in a Rod. To derive an equation for temperature distribution in the rod, and the heat transfer from it, it is necessary first to impose some limitations and assumptions:[12]

1. The heat flow and temperature distribution throughout the rod is independent of the time.

2. The rod material is homogeneous.
3. The heat flow to or from the rod surface at any point is directly proportional to the temperature difference between the surface at that point and the surrounding fluid.
4. The heat transfer coefficient is the same over the entire surface.
5. The temperature of the fluid surrounding the rod is uniform.
6. The temperature of the wall is constant.
7. The rod diameter is so small compared with its height that temperature differences in any cross-sectional area of the rod are negligibly small.
8. The heat transfer through the outermost edge of the rod is negligible compared with that passing into the rod through its sides.

Heat flow at any cross-section in the rod is

$$Q_k = -kA\frac{dt}{dx} \qquad \text{Eq. 54}$$

where the negative sign indicates that the temperature decreases in the x direction.

If t_g is the fluid temperature, the heat given up by the differential surface dx is

$$Q_c = h_f (P dx)(t - t_g) \qquad \text{Eq. 55}$$

where t is the surface temperature at distance x.

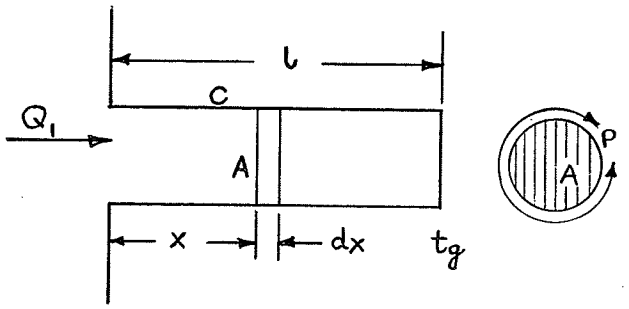

Figure 8. Steady heat conduction in a rod.

As the consequence of this heat loss, there is less heat flowing along the rod with increasing distance x, and thus, through the cross-section $(x+dx)$, the heat flow is

$$Q_k' = Q_k + dQ_k \qquad \text{Eq. 56}$$

or

$$Q_k' = \frac{-kA\,dt}{dx} - kA\,\frac{d^2t}{dx^2}\,dx \qquad \text{Eq. 57}$$

But in a steady state the difference between Equation 54 and Equation 57 must be equal to Equation 55.

Therefore

$$-kA\,\frac{dt}{dx} + \frac{kA\,dt}{dx} + \frac{kA\,d^2t}{dx^2}\,dx = h_f P dx\,(t-t_g) \qquad \text{Eq. 58}$$

Thus the differential equation

$$h_f P (t - t_g) = k A \frac{d^2 t}{d x^2} \qquad \text{Eq. 59}$$

is derived. If the symbol $\theta = t - t_g$ and $m^2 = \frac{h_f P}{k A}$ is used, Equation 59 becomes

$$m^2 \theta = \frac{d^2 \theta}{d x^2} \qquad \text{Eq. 60}$$

The general solution of the differential Equation 60 gives

$$\theta = B_1 e^{-mx} + B_2 e^{mx} \qquad \text{Eq. 61}$$

where B_1 and B_2 are constants of integration, whose values must be determined from the boundary conditions. One of the boundary conditions is that at $x = 0$, the rod temperature is t_o, or $\theta = \theta_o$. To obtain a solution satisfying this condition, we substitute it in Equation 61 and get

$$\theta_o = B_1 e^{-o} + B_2 e^{o} = B_1 + B_2 \qquad \text{Eq. 62}$$

To obtain the second boundary condition, we use the eighth assumption (page 36). Thus,

$\frac{dt}{dx} = \frac{d\theta}{dx}$ at $x = l$. Differentiating Equation 61 and inserting this condition, we get

$$e^{2ml} = \frac{B_1}{B_2} \qquad \text{Eq. 63}$$

Substituting the expression for B_1 from Equation 63 into Equation 62, we obtain

$$B_2 = \frac{\theta_o}{1 + e^{2ml}}$$

and

$$B_1 = \frac{\theta_o}{1 + e^{-2ml}}$$

Substituting the values for the constants B_1 and B_2 in Equation 61, we obtain

$$\theta = \theta_o \left(\frac{e^{ml} e^{-mx} + e^{-ml} e^{mx}}{e^{ml} + e^{-ml}} \right)$$ and simplifying

we obtain

$$\theta = \theta_o \frac{\cosh m(l-x)}{\cosh ml} \qquad \text{Eq. 64}$$

The heat flow rate from the rod is then found to be

$$Q_1 = -kA \left(\frac{d\theta}{dx}\right)_{x=0} = mkA\theta_o \tanh ml \qquad \text{Eq. 65}$$

2. Temperature Distribution in Rectangular Fins. The straight rectangular fin (Figure 9) can be treated by the same methods as those used for the rod.

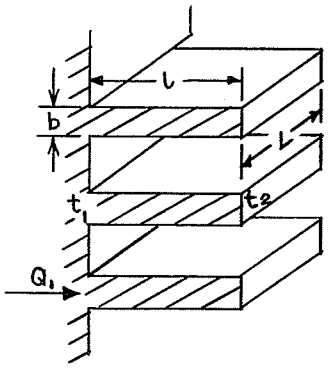

Figure 9. Rectangular fin nomeclature for a plane wall.

Using the symbols in Figure 9, the cross-sectional area of the fin is bL and the circumference P is $2L$, when b is small compared with L.

Therefore, for rectangular fins $m = \sqrt{\frac{2h_f}{kb}}$ is to be used in Equations 64 and 65. As long as the height of the fins on a tube is comparatively small, the formula derived for the plane wall can also be used for the cylinder.

3. Temperature Distribution in Triangular Fins. The triangular fin is of practical interest because it very closely approximates the shape yielding the maximum heat flow per unit weight.[16]

The derivation of the differential equation for the temperature distribution in a triangular fin is similar to the one performed for the rod. The solution of this equation states that

$$\frac{\theta}{\theta_o} = \frac{I_o(2B\sqrt{x})}{I_o(2B\sqrt{L})} \qquad \text{Eq. 66}$$

where: $I_o(2B\sqrt{x})$ and $I_o(2B\sqrt{L})$ are modified zero order Bessel functions of the first kind. Selected values of $I_o(2B\sqrt{x})$ and $I_o(2B\sqrt{L})$ are tabulated in reference 16; $z = 2B\sqrt{x}$; and $B = \sqrt{\frac{2Lh_f}{kb}}$.

For the rest of the symbols refer to Figure 10.

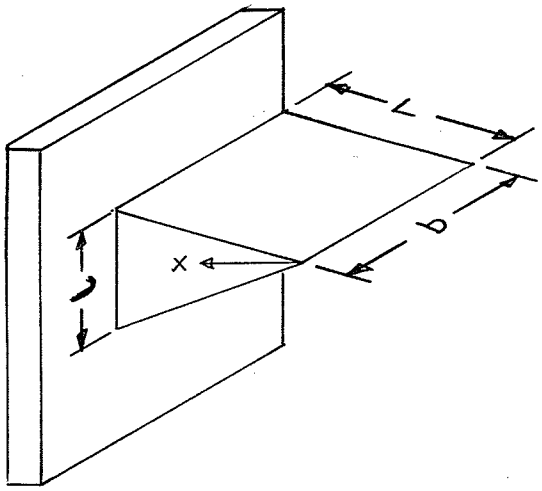

Figure 10. Triangular fin nomeclature.

The rate of heat flow from the fin may be given as

$$Q_1 = \sqrt{2 h_f k b}\ \Theta\ \frac{I_1(2B\sqrt{L})}{I_0(2B\sqrt{L})} \qquad \text{Eq. 67}$$

where $I_1(2B\sqrt{L})$ is a Bessel function as given in reference 16.

b. Fin Efficiency

To calculate the over-all thermal performance of finned surfaces, the temperature gradient along the extended surfaces must be considered. The unfinned portion of the surface is at the wall temperature and transfers heat at 100 per cent efficiency. The heat transfer to or from the fins is by convection, but since the temperature varies along the fin, its surface is not 100 per cent efficient. Thus, we can define a fin efficiency, η_f, as the ratio of the actual fin heat transfer to the heat, which would be

transferred if the entire surface of the fin was at the base temperature.

Thus, for a longitudinal fin of rectangular cross-section[12]

$$\eta_f = \frac{\tanh mb}{mb} \qquad \text{Eq. 68}$$

The fin efficiency, η_f, for other types of fins is given by Gardner[17] in the form of curves.

The effective heat transfer area to be used in calculation of the total heat flow from a finned tube is

$$A_T = A_p + A_f \eta_f \qquad \text{Eq. 69}$$

where A_p is the area of the unfinned portion of the tube and A_f is the area of the fins.

c. Evaluation of the Convective Heat Transfer Coefficient for Fluids Flowing Parallel to Finned Tubes.

As already stated, it is extremely difficult to develop mathematically an expression for the convective heat transfer coefficient for the flow over extended surfaces. Thus, convective heat transfer coefficients for double pipe extended surfaces are computed in the same manner as the coefficients for the annulus flow, that is, the equations developed from dimensional analysis for fluid flow in pipes are used together with a fin efficiency, η_f, and a proper equivalent diameter, D_e.

PART TWO

EXPERIMENTAL EQUIPMENT

a. Reasons for Designing this Type of a Rig

As previously stated, there is practically no available information on heat transfer coefficients for air flowing over the helically finned tubes. For this reason, it has been decided to run a test on a helically finned tube heat exchanger. Since radial temperature gradient in a fin, was one of the items which could be investigated and because, the only available method for measuring this temperature gradient was by the use of thermocouples, the fin had to be of considerable thickness--at least 1/16 of an inch.

After various methods of making the finned tube were disregarded (as for example: cutting the fins on a milling machine from a solid bar), it was decided to weld a 3 1/8-inch outside diameter helical conveyor flight (Figure 11a) on a 1 1/8-inch outside diameter tube. The pitch of the conveyor flight was 3 1/8 inches, with a triangular cross-sectional area, 1/8 inch at the base. Since, with this pitch the spacing between fins would be 3 1/8 inches, only three flights were welded uniformly on the circumference of the 1 1/8-inch tube. It was technically impossible to weld more than three flights because of the minimum space necessary

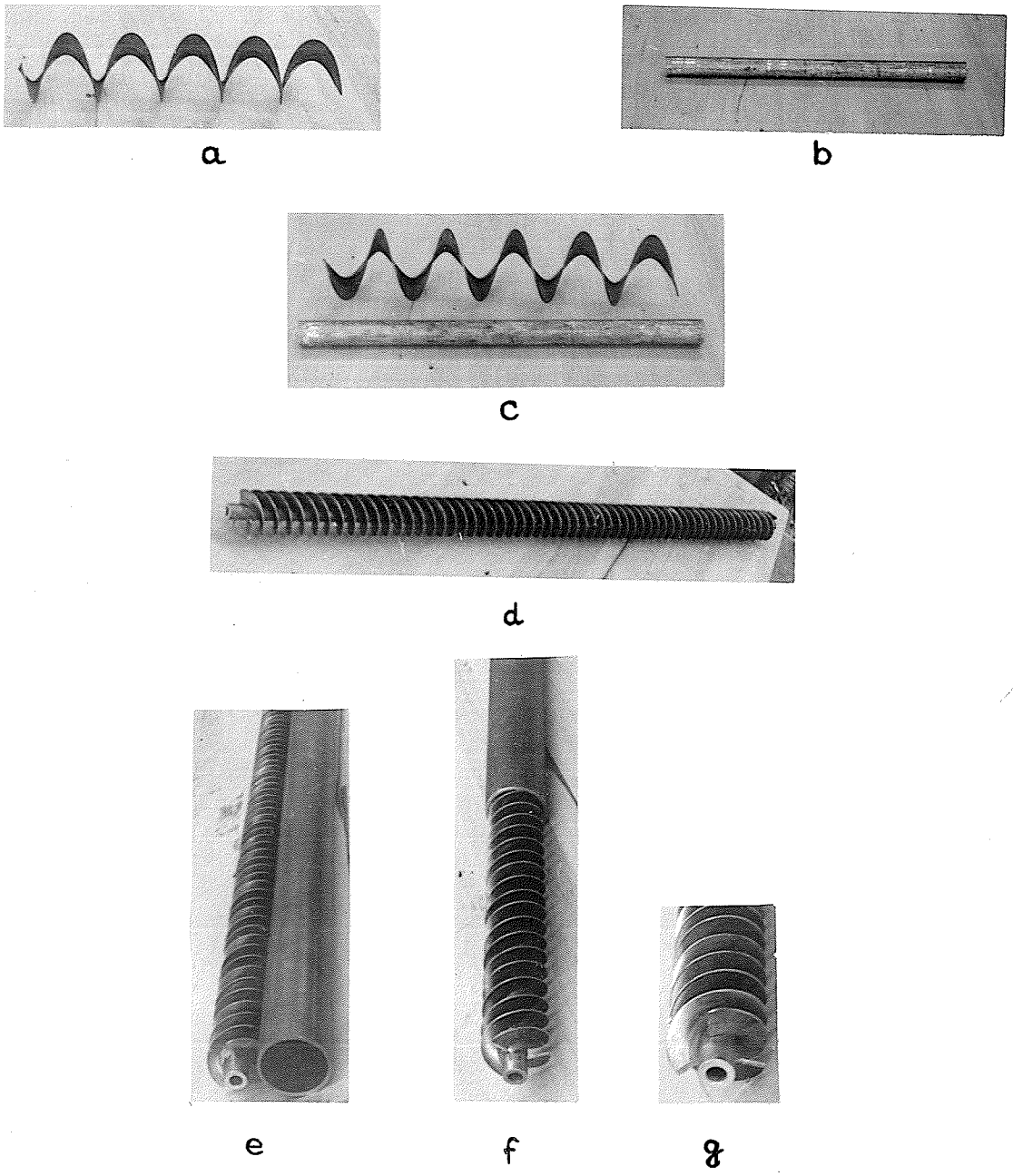

Figure 11. Construction of the finned tube rig.

for welding. For the pictorial explanation of the construction of the finned tube see, Figures 11a-b.

b. Construction of the Rig

The length of the finned tube was five feet (Figure 11d). The flights were welded to the tube on one side only, except for the centre portion, just over the twelve inch calrod heater, where the welding was done on both sides, to ensure better heat transmission.

After the welding operation, the electric heater of 5/8-inches O.D. and 1 kilowatt capacity was fitted inside the finned tube (Figure 12).

To measure the wall temperature of the finned tube, nine insulated thermocouples were imbedded in grooves and silver-soldered into position. The thermocouples were then taken axially along the tube for a minimum length of at least two inches. Then they were inserted through a hole in the wall of the finned tube, to be taken out through the hollow diameter to the rotary switch (Figure 12).

Two fins at the centre of the rig were instrumented with four thermocouples to measure the radial temperature gradient. Each of the thermocouples: No. 1, No. 2, and No. 3 were connected in parallel to give an average reading for the station. Thermocouples No. 4 and No. 7, No. 5 and No. 6 were placed 180 degrees apart on the circumference of

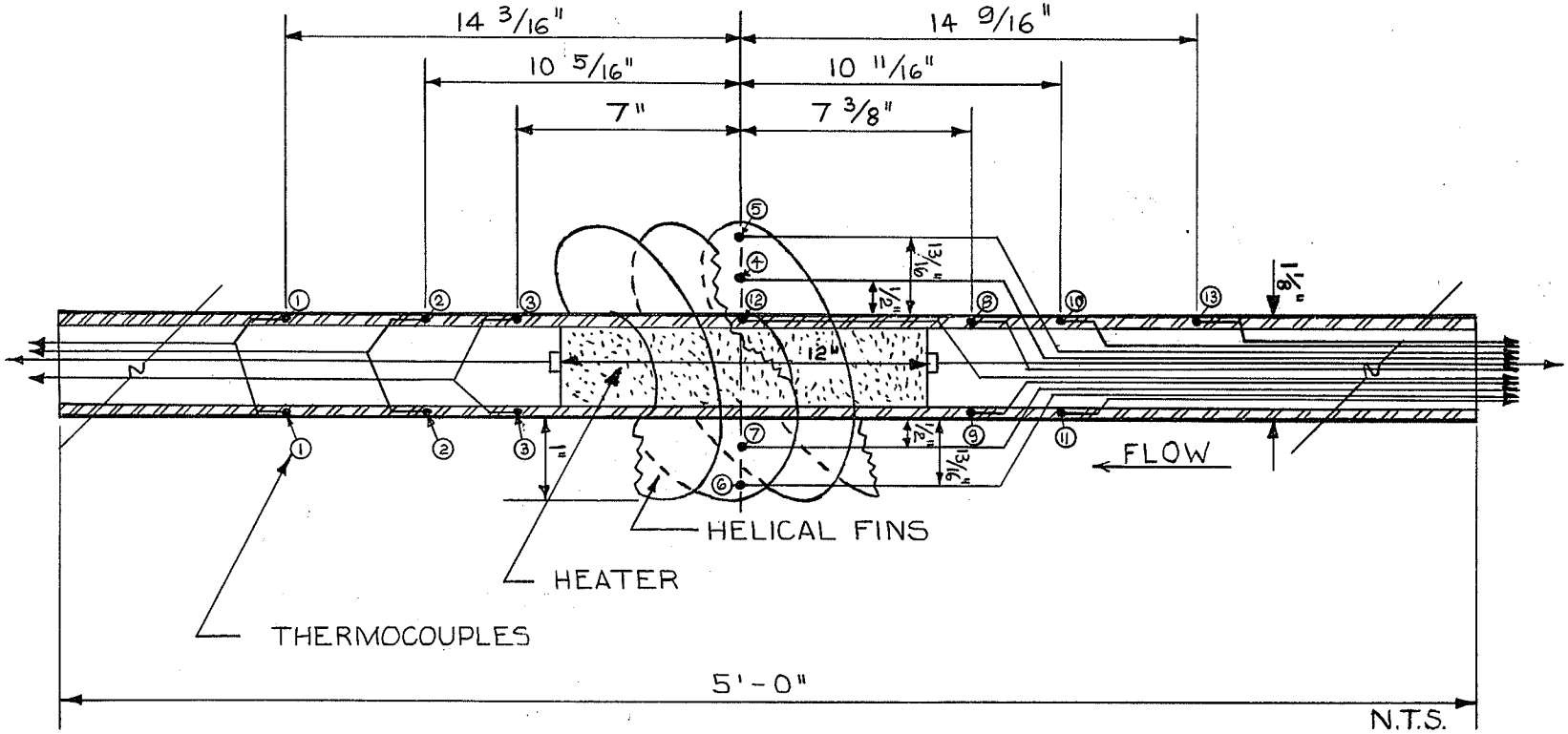

Figure 12. Schematic representation of the finned tube with thermocouples.

the fins while No. 8 and No. 9, No. 10 and No. 11 were similarly attached to the wall of the tube, (Figure 12).

At this time flanges were welded to the larger tube at both ends, and 3/16-inch diameter holes were drilled along its length. Short tubes of 3/16-inch I.D. were welded over these holes, so that the thermocouple probes, used for measuring the temperature of the air, could be moved in and out through the short tubes, (Figure 13).

After this welding operation was accomplished, the finned tube was fitted inside the larger tube (Figure 11f) and then the whole rig was externally lagged to reduce heat losses.

Figure 14 shows the rig bolted to the settling tank, which in turn, through a series of duct work, was connected to "Sir Godfrey" single-staged centrifugal compressor, driven by a diesel through a variable speed hydraulic coupling. The centrifugal compressor supplied air at 0.5 psig — 7.5 psig, depending on what speed the compressor was run.

A stand supported the exit end of the rig. Thermocouples No. 1, No. 2, No. 3, and the power cable was taken out through the exit end of the rig, while the rest of the thermocouples and the second power cable were taken out through the entrance end of the rig, (Figure 12).

In the settling tank, at the rig entrance, a thermometer provided a check on the temperature of the incoming air and a

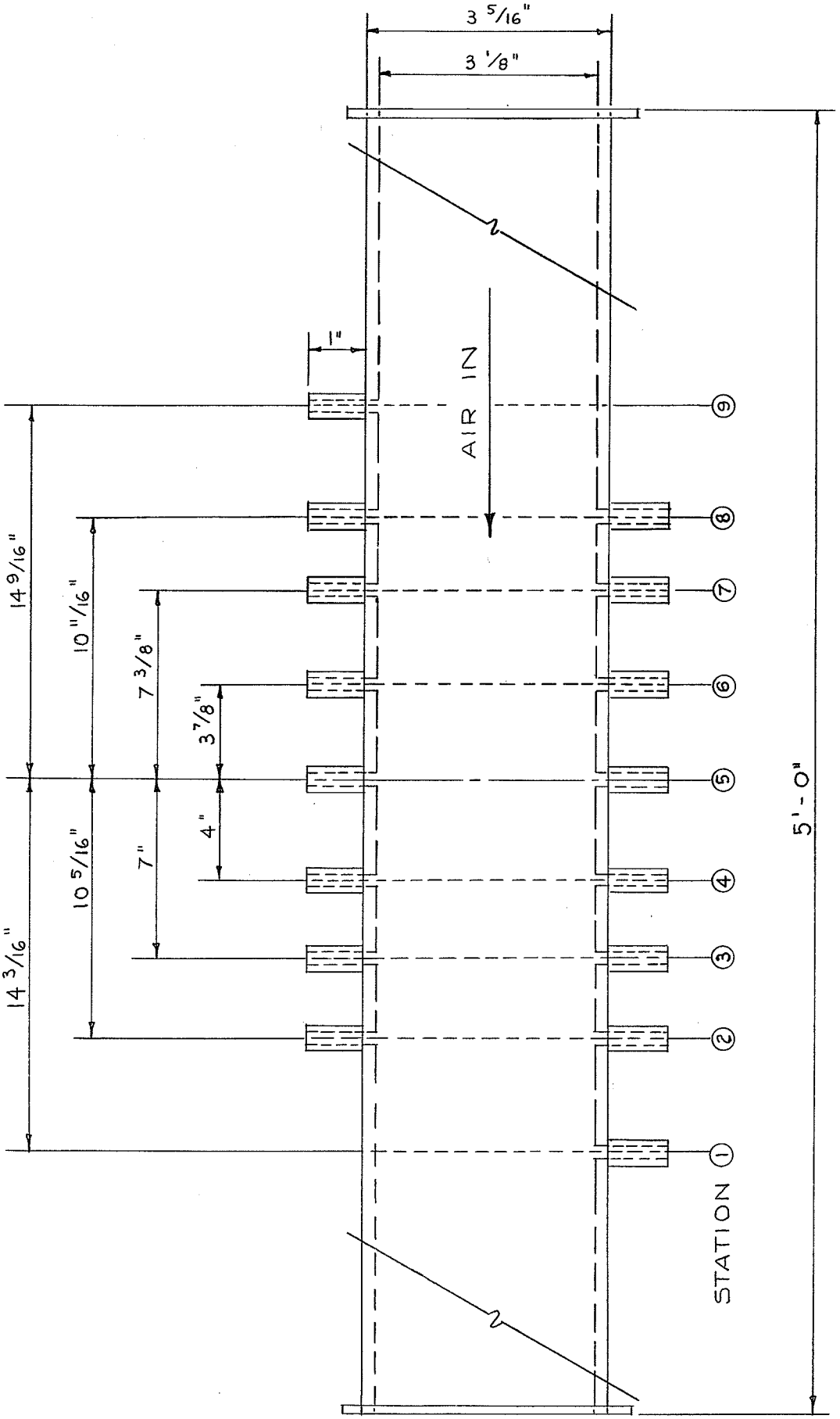

Figure 13. The outside tube.

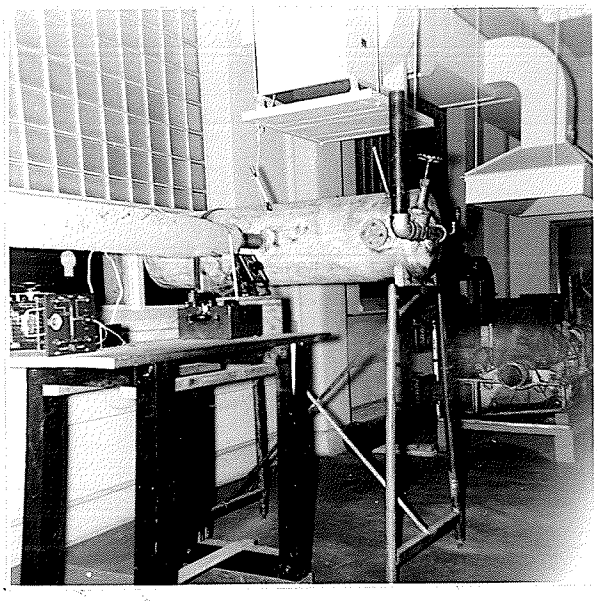

Figure 14. The rig with instruments.

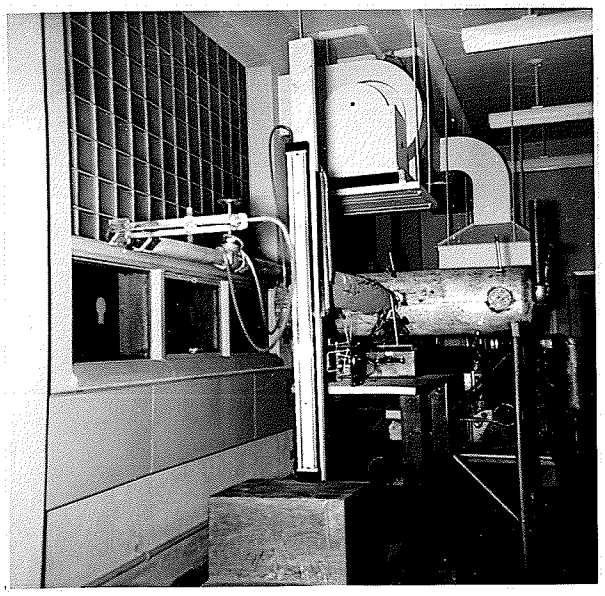

Figure 15. The impact tube and the manometer.

gauge indicated its pressure. The settling tank was also provided with a valve, so that the supply of air to the rig could be regulated without changing the speed of the compressor.

c. Instrumentation

1. Mass Flow Measurements. The velocity pressure was measured with an impact tube and a water manometer at the exit end of the rig, (Figure 15). Knowing the room temperature, the temperature of the outgoing air and the cross-sectional area, the mass flow, M, could be calculated, (as in Table II in Appendix C).

The readings obtained with this impact tube corresponded very closely with those obtained with a smaller impact tube.

2. Temperature Measurements. Iron-constantan thermocouples were used to measure the temperature of the air, the temperature of the tube wall and the temperature of the fins. The thermocouples were connected to a rotary switch, and the e.m.f. was measured with a Brown Instrument Company potentiometer, having a range from 0-60 M.V.

3. Heat Flux Measurements. The power supplied to the calrod heater was measured with a Weston Electric wattmeter having a range from 1-1.5 kilowatts on one scale, and 1-3 kilowatts on a second scale. A variac adjustable transformer was used to adjust the power input to the heater.

PART THREE

TEST PROCEDURE

The diesel engine was always started at least one half-hour before each test, to ensure steady conditions. The speed of the compressor was then set to give the required mass flow. The transformer was then adjusted until the heater output was one kilowatt. Thermocouple No. 12 was always checked for uniform conditions during an interval of ten minutes, before any readings were taken.

Usually two impact tube traverses were taken during a test, together with the room temperature and the outgoing air temperature.

Temperature measurements of the tube wall and the fins were taken in successive order, starting with the temperature at station one up to station nine. Regular checks for steady conditions of thermocouple No. 12 were made. After the above set of temperature readings was taken, the temperature of the air was recorded.

At each station, there were two probes, 180 degrees apart, connected in parallel, to measure the average air temperature. The cross-sectional area of the rig was divided into three equal areas, and the air temperature measurements were made at the centre of each area (similarly

to a pitot tube measurements in a duct). The average of the three readings was used as the average temperature of the air at a station. The air temperature readings were taken in successive order, starting at station one.

Since there were no thermocouples imbedded in the tube wall at stations four and six, a special thermocouple probe was designed to measure these tube wall temperatures. This probe was inserted through the openings, provided for air temperature measurements, to obtain apparent tube wall temperatures for stations four, five and six. Now for station five, two temperatures were known (thermocouple No. 12 gave one temperature). Since it was assumed that the difference between these two temperatures is the same as the difference between the true tube wall temperature and the apparent one at stations four and six, it was now possible to calculate the true tube wall temperatures at these two stations.

Similarly, a second set of readings for the tube wall, the fin and the air temperatures was obtained.

Whenever there were two thermocouples, 180 degrees apart at a station, an average of the two readings was used in the calculation.

After one test was completed, the valve on the settling tank was adjusted to increase the flow of air through the rig. If this adjustment was not sufficient to give the necessary flow of air, then the speed of the compressor had

to be increased to give this flow. Because the increase in the compressor's speed increased the temperature of the incoming air, about thirty minutes had to be allowed after every speed change before a new steady state condition could be reached in the rig.

The procedure outlined above was repeated for each successive test.

PART FOUR

PRESENTATION OF RESULTS

An average of the readings taken during the test can be found in Tables I - V, Appendixes B and C. The mass velocity of air, G, at the test section was calculated from the weight flow, w, and the cross-sectional area. (Table III, Appendix C). From the mass velocity, the equivalent diameter, D_e, and viscosity, μ, the Reynolds number, N_{Re}, was obtained (see Sample Calculation, Appendix C).

Two convective heat transfer coefficients were calculated: the "effective" local heat transfer coefficient, h_{fx}, for station five, and the "effective" average heat transfer coefficient, h_{fa}, between stations four and six. The "effective" local heat transfer coefficient was obtained from the total power input, divided by the "effective" heat transfer area times the difference between the average air and the tube wall temperature at station five (see Explanation, Appendix C). Similarly, the "effective" average heat transfer coefficient was obtained, except that the logarithmic temperature difference between the tube wall temperature and the average air temperature between stations four and six was used. To calculate the heat transfer area for the above two coefficients, it was assumed that the twelve inch heater supplied all of its 3,415 B.T.U. to the

air, with no losses to the surroundings. The results obtained for the two coefficients are presented in Tables III and IV, Appendix C.

After the two coefficients were calculated, $N_{Nu} / (N_{Pr})^{\frac{1}{3}}$ vs. Reynolds number was plotted, and thus the constant C , and the exponents x and y for Equation 46 were obtained (Figures 16 and 17, Appendix C).

Further, the local and average Stanton numbers were obtained from the local and the average "effective" heat transfer coefficients respectively, and the results presented in Tables III and IV, as well as in Figures 18 and 19, Appendix C.

Two other coefficients, h'_{fx} , and, h'_{fa} , based on hundred per cent efficiency of the fins, were calculated. The results obtained are given in Table V, Appendix C. Figures 16 and 17, Appendix C give the graphs of $N_{Nu}/(N_{Pr})^{\frac{1}{3}}$ vs. N_{Re}, based on h_{fx} and h_{fa} respectively. Also, an average coefficient between stations four and six, based on both hundred per cent efficiency of the fins and the heat balance on air flowing in the rig, was calculated and presented in Table VI, and then the graph of $N_{Nu}/(N_{Pr})^{\frac{1}{3}}$ vs. N_{Re} was plotted in Figure 17, Appendix C.

Since the actual flow area in a helically finned tube exchanger is the area at right angle to the fins (see Calculations in Appendix C), a new equivalent diameter, d_e,

based on this flow area, was used to calculate the new average Nusselt number between stations four and six. The convective coefficient, h, in this Nusselt number was obtained from the heat balance on the air flowing between stations four and six. A new Reynolds number, based on d_e, was calculated, and $N_{Nu}/(N_{Pr})^{\frac{1}{3}}$ vs. N_{Re} plotted in Figure 20.

The radial temperature gradients in the fin at station five were calculated from Equation 66, using the "effective" local heat transfer coefficients. The comparison of the above results with the temperature gradients, as obtained with thermocouples No. 4, No. 5, No. 6 and No. 7, can be found in Table VIII, Appendix C.

PART FIVE

DISCUSSION OF RESULTS

a. Error Analysis

Since the measured and calculated heat transfer coefficients differ, the factors involved in the tests must be examined.

The heat input was determined from the wattmeter readings. The error in the instrument was one-half of one per cent of the full scale deflection.

The error in the temperature measurements was quite large, probably in the vicinity of 3° F. The thermocouples were imbedded in grooves in the tube and silver-soldered into position. The deposition of a different metal introduced a new junction, and thus, increased the error. On the other hand, since all the thermocouples were soldered into position by the same person, who paid special attention to deposit as little silver solder as possible, and since temperature differences were used in the calculations, the error was minimized.

There was some heat loss due to conduction from the tips of the fins to the outside tube. These conduction losses lowered the temperatures on the tube and the fins, and increased the convective heat transfer coefficients.

The e.m.f. measurements were made with a potentiometer

that could be read with an accuracy of $\pm$ 0.01 m.v., that is, about $\pm 0.33^{\circ}$ F.

Since the manometer used in this test had only ten divisions per inch, the height of the water column could not be read very accurately at the lower mass flow. This introduced an error in mass velocity and Reynolds number calculations.

b. Discussion of the Data Obtained

Limited time prevented a large number of runs from being taken. The tests points fell in the range of Reynolds numbers from 2.34×10^4 to 1.11×10^5 when conventional equivalent diameter, D_e , was used. Since it was hard to read the manometer accurately at low mass flow of air, no tests were performed at a lower Reynolds number than 2.34×10^4 as already explained. The compressor speed, which gave us the Reynolds number of 1.11×10^5, was the maximum speed at which it could be run. Higher speeds resulted in compressor surge.

As can be seen from Table II, Appendix C, the temperature of air at the rig exit varied from 107° F. to 219° F. throughout the twenty tests performed. This was due to the fact that in increasing the speed of the compressor, air was compressed more and thus its temperature increased.

c. Discussion of the Results Obtained

As can be seen from Table VIII, Appendix C, there is

some difference between the obtained and the calculated temperature gradient in the fin at station five. Probably the thermocouples were not silver-soldered exactly at the required radial distance from the tube, and thus the two temperature gradients differ. On the whole, the obtained temperature gradients compared favourably with the calculated temperature gradients. This suggests that the theoretical formula for the radial temperature gradient is in close agreement with the actual results.

Figure 16 gives the heat transfer curves at station five. The slope of the best straight line through the points, based on effective heat transfer coefficient and the total power input, is very close to 0.8 and the constant C (Equation 46) is 0.07. The slope of the best straight line through the points, based on hundred per cent efficiency of the fins and the total power input is 0.64 and the constant C is 0.27. For any Reynolds number, curve 1 and curve 2 give a higher $N_{Nu}/(N_{Pr})^{\frac{1}{3}}$ than the curve calculated from Equation 51. (The term $\left\{\frac{\mu}{\mu_w}\right\}^{0.14}$ was close to unity and therefore was omitted in the calculation.)

Similarly, from Figure 17, the slope of the best straight line through the points, based on effective heat transfer coefficient and the total power input, is 0.8 and the constant C is 0.072. The slope of curve 2 in Figure 17 is 0.65 and the constant C is 0.25. Both curves again give

higher $N_{Nu}/(N_{Pr})^{\frac{1}{3}}$ than the curve based on Equation 51.

As can be seen from curves 1 and 2 in Figures 16 and 17, the points at the lower Reynolds number do not fall close to the curves. Probably, the impact tube readings at the lower flow introduced an error in the Reynolds number and the mass flow calculations.

The curves, based on total power input, give much higher results of N_{Nu} than the curve, based on Equation 51. The reason for this is that, in using the total power input we introduced an error in the calculation. There was some end conduction in the finned tube (as can be seen from the temperature distribution in the finned tube, Table Ia), which decreased the power input to the test section. Thus corrected total power input should have been used in the calculations of $N_{Nu}/(N_{Pr})^{\frac{1}{3}}$ for Figures 16 and 17. It was not attempted to correct for this end effect, but a new $N_{Nu}/(N_{Pr})^{\frac{1}{3}}$ based on heat balance between stations four and six was calculated.

Curve 1 in Figure 21, based on heat balance and hundred per cent efficiency of the fins, agrees very closely with the curve obtained from Equation 51. Curve 2 in Figure 21, based on heat balance and the effective heat transfer coefficient, has a slope of 0.8 and the constant C of 0.038.

Thus, $N_{Nu}/(N_{Pr})^{\frac{1}{3}} = 0.038\ N_{Re}^{0.8}$ can be used in the

design of helically finned tube rigs, provided the proper equivalent diameter, D_e , and the efficiency, η_f , is used in the calculation. However, there is no assurance that the above equation will prove correct for finned tube rigs of different dimensions and design.

The curves of the local and average Stanton Number vs. Reynolds Number are presented in Figures 18 and 19 respectively. It is difficult to compare the above curves with the curves presented by E. W. V. Acton in Atomic Energy Review.[3] Since in his rig, air was flowing in an annulus between the fins and the channel, he defined his equivalent diameter as the difference between the channel diameter and the fin tip diameter. The above definition of the equivalent diameter cannot be applied to this rig, because in this case, there is no annular space between the fins and the outside tube. On the other hand, if the curves of Stanton Number vs. Reynolds Number, as presented in Figures 18 and 19, are compared with the curves presented by Acton, one can see a close agreement between them (in the range of Reynolds Number considered), even though, each is based on a different definition of the equivalent diameter.

Since the actual flow area in a helically finned tube exchanger is the area at right angle to the fins (see Appendix C), a new equivalent diameter, d_e , based on this flow area, was introduced. For a helically finned tube rig, the

equivalent diameter, as defined above, seems to be quite appropriate, and if tried with other helically finned tube rigs it might correlate the convective coefficient better than the equivalent diameter D_e .

The results obtained for $N_{Nu}/(N_{Pr})^{\frac{1}{3}}$, using d_e, are given in Table VII. The curve of $N_{Nu}/(N_{Pr})^{\frac{1}{3}}$ vs. N_{Re} is plotted in Figure 20. The slope of the above curve, based on hundred per cent efficiency, and heat balance between stations four and six, is 0.8 and the constant C is 0.022. The slope of curve 3, based on effective heat transfer coefficient and heat balance between stations four and six, is 0.8 and the constant C is 0.027.

It is interesting to compare the results obtained for the convective coefficients when based on d_e and D_e. The coefficients obtained using equivalent diameter, d_e, are about 40 per cent lower than the coefficients obtained when equivalent diameter, D_e , is used. Since only one fluid was used with this rig, it is impossible to know which of the two equivalent diameters gives a better correlation of the convective coefficient.

It is felt that some more work could be done on this particular finned tube rig. Pressure drops, as well as heat transfer coefficients, based on heat transferred in the passages formed by the fins, could be calculated.

Also, a new rig could be designed, using the same

finned tube. The finned tube could be placed in an annulus in such a way, so that some flow area remained between the fins and the outside tube. Heat transfer curves, for the above design, could then be compared with the curves obtained at present.

Since the rig was not leakproof, no liquid could be used as the heat transfer medium. A similar new rig could be designed, but in such a way that liquids, as well as air, could be used in it. This would permit to correlate the convective coefficients of different fluids, based on d_e and D_e. Only then, a statement could be made which of the equivalent diameters gives a better correlation of the convective coefficient.

PART SIX

SUMMARY

Heat transfer coefficients were determined for air "flowing over" a hellically finned tube. The tube was heated internally with an electric calrod heater, whose output was kept constant at 1 kilowatt. The tests were performed in the range of Reynolds numbers from 2.34×10^4 to 1.11×10^5. The average and the local Stanton numbers were calculated and plotted against the Reynolds numbers. Equation of the form $N_{Nu}/(N_{Pr})^{\frac{1}{3}} = 0.038\ N_{Re}^{0.8}$ was obtained, using the equivalent diameter D_e. The values obtained for the term $N_{Nu}/(N_{Pr})^{\frac{1}{3}}$, when the equivalent diameter d_e and the effective heat transfer coefficients were used, were about 40 per cent lower than the values when the equivalent diameter D_e was used. Radial temperature gradients in the fin at station five compared favourably with the theoretical temperature gradients.

REFERENCES

REFERENCES

1. Griffiths, E. and J. H. Awbery. "Heat Transfer Between Metal Pipes and a Stream of Air." The Institution of Mechanical Engineers Proceedings, 1933. London, England.

2. DeLorenzo, B. and E. D. Anderson. "Heat Transfer and Pressure Drop of Liquids in Double Pipe Fintube Exchangers." A.S.M.E. Transactions, Vol. 67, 1945. New York.

3. Acton, E. W. V. "Heat Transfer." Atomic Energy Review, Sept., 1957.

4. Giedt, W. H. Principles of Engineering Heat Transfer. First edition. Toronto-New York-London: D. Van Nostrand Co. Inc., 1957.

5. Schlichting, H., Dr. Boundary Layer Theory. New York: McGraw-Hill Book Co. Inc., 1955.

6. Eckert, E. R. G. and R. M. Drake, Jr. Introduction to the Heat Transfer and Mass. New York: McGraw-Hill Book Co. Inc., 1950.

7. Kays, W. M. "Numerical Solutions for Laminar-Flow Heat Transfer in Circular Tubes." A.S.M.E. Transactions, 1945.

8. Jakob, M. Heat Transfer. Vol. I. New York: John Wiley and Sons, Inc., London: Chapman and Hall, Ltd., 1957.

9. Brown, A. I. and S. M. Marco. Introduction to Heat Transfer. Third edition. New York and London: McGraw-Hill Book Co. Inc., 1958.

10. McAdams, W. H., Heat Transmission. Second edition. New York and London: McGraw-Hill Book Co. Inc., 1942.

11. Miller, P., J. J. Byrnes and D. M. Benforado. "Heat Transfer to Water Flowing Parallel to a Rod Bundle." A.S.M.E. Transactions, 1955. New York.

12. Kern, D. Q. Process Heat Transfer. New York, Toronto, London: McGraw-Hill Book Co. Inc., 1950

13. Perry, J. H. Chemical Engineers' Handbook. Second edition. New York: McGraw-Hill Book Co., Inc.

14. Donohue, D. A. Ind. and Eng. Chemistry. V. 41, November, 1949.

15. Schenk, H., Jr., Heat Transfer Engineering. Englewood Cliffs: Prentice-Hall, Inc., 1959.

16. Kreith, F. Heat Transfer. Scranton: International Textbook Co., 1958.

17. Gardner, K. A. "Efficiency of Extended Surfaces." A.S.M.E. Transactions, Vol. 67, 1945.

APPENDIX A

APPENDIX A

Use of Cubic Parabola to Develop an Expression for the Boundary Layer Thickness:

A fully developed boundary layer has a shape as indicated in figure 6, page 17. To solve the theoretical equations for the boundary layer thickness and the shearing stress the shape of the velocity profile must be defined. Numerous experimental measurements have been made and the actual velocity profiles are known for several types of flow, including longitudinal flow over a flat plate.

To fit the theoretical equations to the experimental results the following conditions must be satisfied:

At $y = 0$ $\quad u = 0$

$\frac{\partial^2 u}{\partial y^2} = 0$ for laminar sub-layer

At $y = \delta$ $\quad u = u_\infty$

and $\frac{\partial u}{\partial y} = 0$ for smooth joining of the curve.

For further accuracy the second, third and higher derivatives could be placed equal to zero at $y = \delta$, but the four conditions listed above are generally taken as sufficieht and the velocity profile can then be approximated by:

$$u = a + by + cy^2 + dy^3$$

Applying the conditions listed yields:

$a = 0$, $\quad b = \frac{3}{2}\frac{u_\infty}{\delta}$, $\quad c = 0$ and $d = -\frac{1}{2}\frac{u_\infty}{\delta^3}$

or $u = by + dy^3$

and the integration of equation 23 proceeds as follows:

$$u_\infty^2 \int_0^\delta \left\{\frac{3}{2}\frac{y}{\delta} - \frac{1}{2}\left(\frac{y}{\delta}\right)^3\right\}\left\{1 - \frac{3}{2}\frac{y}{\delta} + \frac{1}{2}\left(\frac{y}{\delta}\right)^3\right\} dy$$

$$= u_\infty^2 \int_0^\delta \left(\frac{3}{2}\frac{y}{\delta} - \frac{9}{4}\frac{y^2}{\delta^2} - \frac{1}{2}\frac{y^3}{\delta^3} + \frac{3}{2}\frac{y^4}{\delta^4} - \frac{1}{4}\frac{y^6}{\delta^6}\right) dy$$

$$= u_\infty^2 \left(\frac{3}{2}\frac{1}{\delta}\int_0^\delta y\,dy - \frac{9}{4}\frac{1}{\delta^2}\int_0^\delta y^2 dy - \frac{1}{2}\frac{1}{\delta^3}\int_0^\delta y^3 dy + \frac{3}{2}\frac{1}{\delta^4}\int_0^\delta y^4 dy - \frac{1}{4}\frac{1}{\delta^6}\int_0^\delta y^6 dy\right)$$

$$= u_\infty^2 \left\{\frac{3}{4}\frac{1}{\delta}\left(y^2\right)_0^\delta - \frac{3}{4}\frac{1}{\delta^2}\left(y^3\right)_0^\delta - \frac{1}{8}\frac{1}{\delta^3}\left(y^4\right)_0^\delta + \frac{3}{10}\frac{1}{\delta^4}\left(y^5\right)_0^\delta - \frac{1}{28}\frac{1}{\delta^6}\left(y^7\right)_0^\delta\right\}$$

$$= u_\infty^2 \left\{\frac{3}{4}\frac{1}{\delta}\left(\delta^2\right) - \frac{3}{4}\frac{1}{\delta^2}\left(\delta^3\right) - \frac{1}{8}\frac{1}{\delta^3}\left(\delta^4\right) + \frac{3}{10}\frac{1}{\delta^4}\left(\delta^5\right) - \frac{1}{28}\frac{1}{\delta^6}\left(\delta^7\right)\right\}$$

$$= \frac{39}{280}\, u_\infty^2 \delta$$

Derivation of Equation 16:

From Eq. 14, $\eta = y\sqrt{\frac{u_\infty}{\nu x}}$ and $d\eta = dy\sqrt{\frac{u_\infty}{\nu x}}$ or $d\eta = \frac{dy}{\delta}$

Since $\frac{u}{u_\infty} = F\left(\frac{y}{\delta}\right)$ and $u = \frac{d\psi}{dy}$,

$$\psi = \int u\,dy = \int u_\infty F\left(\frac{y}{\delta}\right) dy = u_\infty \delta \int F\left(\frac{y}{\delta}\right) d\eta.$$

Let $\int F\left(\frac{y}{\delta}\right) d\eta = f(\eta)$, then $\psi = u_\infty \delta f(\eta)$ and $\frac{d\psi}{d\eta} = u_\infty \frac{\delta\, df(\eta)}{d\eta}$.

Since $u = \frac{d\psi}{dy} = \frac{d\psi}{d\eta}\frac{d\eta}{dy} = u_\infty \frac{\delta\, df(\eta)}{d\eta}\frac{1}{\delta} = u_\infty \frac{df(\eta)}{d\eta} = u_\infty \frac{df}{d\eta}$,

then $$u = u_\infty \frac{df}{d\eta} \qquad \text{Eq. 16}$$

APPENDIX B

TABLE Ia

TUBE WALL TEMPERATURES

Test No.	Thermocouple No. and Tube Wall Temperatures*								
	1	2	3	8	9	10	11	12	13
1	187.9	189.3	231.2	138.6	142.0	126.0	126.3	326.9	125.0
2	173.2	176.8	217.8	138.0	140.2	126.8	129.1	307.1	126.8
3	177.0	179.0	218.0	142.0	144.1	131.6	132.0	305.7	131.0
4	168.3	171.3	205.9	140.7	143.3	132.9	133.9	287.9	132.9
5	126.6	129.3	163.8	97.1	99.1	88.3	88.6	249.0	87.4
6	186.2	190.2	219.2	167.2	169.0	160.6	161.9	292.0	161.7
7	125.4	129.0	156.5	106.1	107.4	100.5	102.3	228.7	104.4
8	183.9	186.9	214.0	166.6	167.2	204.1	204.1	279.9	157.2
9	222.2	225.7	248.2	210.9	211.6	203.9	204.6	306.6	203.0
10	145.0	147.4	172.0	130.0	130.9	124.5	125.1	236.3	124.5
11	171.6	174.6	198.1	160.2	160.6	153.6	152.7	260.5	153.4
12	151.9	154.0	178.8	137.2	137.7	132.0	132.7	240.3	132.0
13	165.5	169.0	192.5	152.0	152.3	145.9	144.4	248.0	145.0
14	216.2	219.7	239.2	202.4	201.7	194.7	193.7	292.0	195.1
15	173.9	178.4	199.7	163.2	163.5	157.6	156.5	257.2	156.0
16	171.8	174.4	196.8	159.3	159.4	153.3	151.5	252.8	151.8
17	170.1	174.2	196.0	161.4	161.7	155.5	154.7	254.2	154.1
18	225.6	228.1	248.9	213.9	213.3	206.6	207.6	302.6	208.6
19	190.0	193.7	213.7	178.9	178.9	174.0	174.0	261.0	167.6
20	110.1	112.4	132.0	99.4	100.1	96.7	96.7	184.3	95.3

Note: Heat input to the heater was 1 kilowatt for all tests.

* All temperatures in ^{o}F.

TABLE Ib

AVERAGE AIR TEMPERATURES

Test No.	Station No. and Average Air Temperatures*								
	1	2	3	4	5	6	7	8	9
1	193.6	190.5	181.6	155.3	141.1	126.1	124.8	123.2	125.0
2	177.1	166.5	163.4	150.0	138.1	127.2	125.3	125.2	125.8
3	177.7	171.3	168.7	151.5	141.2	127.9	125.6	126.8	125.3
4	168.6	167.0	160.2	148.6	139.9	132.4	129.0	127.4	127.4
5	127.0	125.0	121.3	106.8	98.4	88.5	86.3	86.3	85.1
6	189.6	188.9	181.3	171.9	166.7	160.8	160.1	160.3	
7	127.5			110.9	106.0	100.6	99.1	99.0	99.0
8	181.0	181.0	174.4	167.7	163.0	158.0	155.4	154.6	156.0
9	225.0	226.5	219.0	209.5	206.0	202.5	202.0	202.0	202.2
10	144.5			128.6	128.2	123.9	124.0	123.9	123.9
11	175.2	176.8	171.2	161.3	159.1	154.1	154.3	153.7	153.6
12	151.0			138.8	138.8	132.0	131.3	131.1	131.0
13	167.9	171.7	166.2	155.4	152.4	146.6	148.9	147.4	145.4
14	218.4	218.8	214.0	203.4	201.0	197.0	194.5	191.9	193.6
15	178.0	176.9	171.5	163.8	159.7	156.9	155.8	155.2	154.8
16	176.0	176.2		162.2	160.0	154.6	154.6	153.9	153.9
17	173.9	170.8	168.1	161.9	156.6	153.9	153.0	154.2	152.9
18	226.0	224.5	221.5	216.5	213.5	210.8	211.0	210.1	210.9
19	182.7	183.1	176.2	175.1	172.1	169.6	168.6	168.1	168.1
20	105.9	105.8	104.7	102.2	99.6	96.6	90.6	90.2	90.8

* All temperatures in ^{o}F.

APPENDIX C

APPENDIX C

SAMPLE CALCULATIONS, TABLES AND GRAPHS

Calculation of the Reynolds number for Test 1:

$$V_a = \sqrt{2g \frac{d_w h v_a}{12 d_a}}$$

$$V_a = \sqrt{2g \frac{62.3 \times 9.164 \times 10^{-1}}{12 \times 6.279 \times 10^{-2}}} \times 60 = 4010 \text{ f.p.m.}$$

Area at exit $= \frac{\pi D^2}{4} = \frac{\pi}{4} \left(\frac{1.615}{12}\right)^2 = 0.01423 \text{ ft}^2$

$\therefore M = V_a \times A = 4010 \times 0.01423 = 57.1$ c.f.p.m.

$\therefore W = M \times d_a \times 60 = 57.1 \times 6.279 \times 10^{-2} \times 60 = 215$ lbs/hr

Cross-sectional area at the test section = Area of the annulus - Area of fins

$$= \frac{\pi}{4 \times 144}\left(3.125^2 - 1.125^2\right) - \frac{3 \times 1 \times 0.0975}{144} = 0.0464 - 0.001953 = 0.044447 \text{ sq.ft.}$$

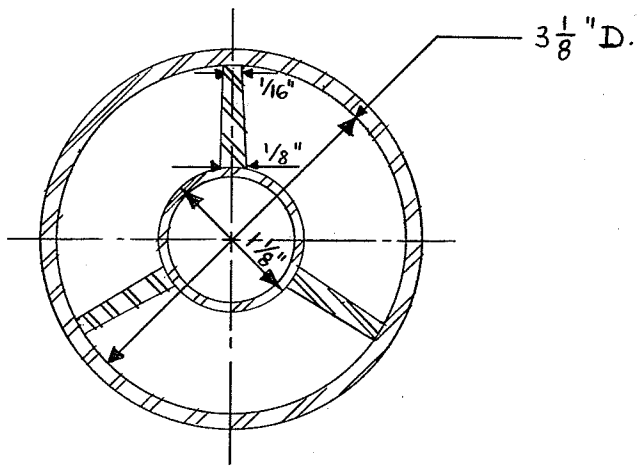

Cross-section of the rig

Say $a_T = 0.04445$ sq.ft.

$G = W \times a_T = 215 \times 0.04445 = 4840$ lbs/hr/sq.ft. (at the test section)

Equivalent diameter,

$$D_e = \frac{4 \cdot \text{flow area}}{\text{wetted perimeter}}$$

Wetted perimeter

$$= \frac{\pi \times 1.125}{12} - \frac{3 \times 0.125}{12} + \frac{3 \times 2 \times 1}{12}$$

$$= 0.294 - 0.03125 + 0.5 = 0.76275 \text{ ft}$$

Say wetted perimeter = 0.76 ft.

$$D_e = \frac{4 \times 0.04445}{0.76} = 0.234 \text{ ft}$$

$$N_{Re} = \frac{G \times D_e}{\mu} = \frac{4840 \times 0.234}{4.84 \times 10^{-2}} = 2.34 \times 10^4$$

Calculation of the "effective" local convective heat transfer coefficient for test 1:

Total effective area = $A_o + \eta_{fx} A_f$

where A_o = Surface area of the bare tube = Area of tube - Area of fins $= \left(\pi \times 1.125 \times 12 - 21 \times 3 \times \frac{1}{8}\right)\frac{1}{144} = 0.2325$ sq. ft.

and A_f = Surface area of fins $= \frac{29.28 \times 2 \times 3}{144} = 1.218$ sq.ft.

and η_{fx} = fin efficiency

but $h_{fx} = \frac{\text{Heat input}}{\Delta t\left(A_o + \eta_{fx} A_f\right)}$

In the above equation we have two unknowns h_{fx} and η_{fx}. The equation is solved by a trial and error substitution. The "effective" local heat transfer coefficient h_{fx} is assumed, and η_{fx} is found from the efficiency curve, given by

Gardner.[17] Then, from the above formula h_{fx} is computed. If it does not check with the assumed h_{fx}, the procedure is repeated.

The values for h_{fx}, η_{fx}, h_{fa} and η_{fa} thus found are recorded in Table III and Table IV in Appendix C.

Calculation of the average convective heat transfer coefficient based on the heat balance of air and hundred per cent efficiency of the fins for test 1:

Since the distance between stations four and six was 7 7/8 inches, the total heat transfer area $a_T = A_o + A_f$

$$A_o = \pi \times 1.125 \times 7.875 = 27.8 \text{ sq. in.}$$

Area of the fin base $= 13.78 \times 3 \times \frac{1}{8} = 5.17$ sq. in

$$A_f = 115 \text{ sq. in.}$$

$$a_T = \frac{27.8 - 5.17 + 115}{144} = 0.9554 \text{ sq. ft.}$$

Therefore

$$h = \frac{1509}{186.2 \times 0.9554} = 8.5 \frac{\text{B.T.U.}}{\text{hr/sq. ft./°F}}$$

Calculation for the new equivalent diameter d_e.

$$d_e = \frac{4 \times \text{flow area}}{\text{Wetted perimeter}}$$

The flow area is calculated from the area available between the fins. It was found graphically that this area is 0.905 square inches at, right angles to the fin. The wetted perimeter, is equal to the arc length between the fins plus the wetted

length of the fins.

Therefore $d_e = \frac{4 \times 0.905 \times 3 \times 12}{144 (.64 \times 3 + 1 \times 2 \times 3)} = 0.143$ ft.

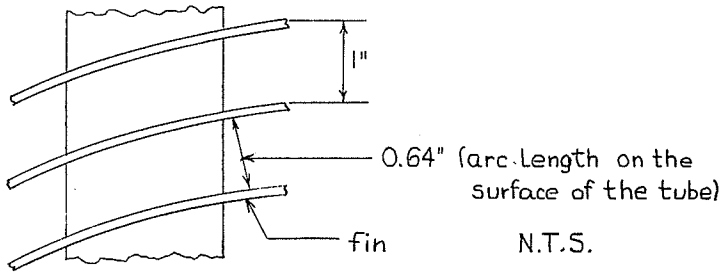

Calculation of the Radial Temperature Gradient at station five:

From Eq. 66, $\frac{\theta}{\theta_o} = \frac{I_o(2B\sqrt{x})}{I_o(2B\sqrt{L})}$, the temperature, t, can be calculated. The symbols are defined as follows:

$\theta = t - t_\infty$; $\theta_o = t_s - t_\infty$; t = temperature at any x ; t_s = temperature at $x = L$; t_∞ = the average temperature of the ambient fluid; $B = \sqrt{\frac{2 L h_f}{k b}}$. The rest of the symbols are defined in nomenclature and in Fig. 10, p. 41.

$I_o(2B\sqrt{x})$ and $I_o(2B\sqrt{L})$ are modified zero order Bessel functions.

Thus from Equation 66 - for test No. 2, at x = 3/16"

$$\frac{t - 138.1}{307.1 - 138.1} = \frac{I_o(2B\sqrt{x})}{I_o(2B\sqrt{L})} \quad ; 2B\sqrt{x} = 2\sqrt{\frac{2 \times 1 \times 18.5}{26 \times 1}} \times \sqrt{\frac{3}{16 \times 12}} = 0.943$$

Similarly $2B\sqrt{L} = 2.18$

$\therefore I_o(2B\sqrt{x}) = 1.237$ and $I_o(2B\sqrt{L}) = 2.54$ (from reference 16)

$$\therefore t_{x=\frac{3}{16}"} = 138.1 + (307.1 - 138.1)\frac{1.237}{2.594} = 138.1 + 80.7 = 218.8\ ^\circ F$$

TABLE II

MASS FLOW AT EXIT

Test No.	Room Temp.*	Air Temp.* at Exit	d_w	d_a $\times 10^{-2}$	$\sqrt{h_{va}}$ $\times 10^{-1}$	V_a	M	W
1	70.0	174.7	62.3	6.279	9.16	4010	57.1	215
2	74.0	167.0	62.26	6.364	11.16	4845	68.9	263
3	73.1	168.0	62.27	6.352	11.88	5170	73.6	281
4	75.1	163.0	62.26	6.417	15.06	6524	92.8	357
5	74.0	127.0	62.26	6.800	13.95	5878	83.6	342
6	80.0	181.5	62.2	6.205	20.83	9175	130.5	486
7	71.0	127.0	62.21	6.786	21.16	8900	126.6	515
8	80.0	177.8	62.2	6.250	24.21	10660	151.6	569
9	89.0	214.0	62.11	5.888	31.64	14210	202.0	713
10	75.0	140.0	62.23	6.630	28.01	11920	169.7	674
11	81.2	168.0	62.20	6.353	30.91	13440	191.0	729
12	79.0	146.0	62.20	6.558	30.07	12880	182.0	716
13	86.0	161.0	62.14	6.430	31.65	13710	195.0	753
14	89.3	208.7	62.11	5.930	35.93	16170	230.0	818
15	82.7	170.3	62.17	6.326	33.41	14560	207.0	786
16	87.0	168.0	62.13	6.352	33.44	14640	208.5	795
17	86.0	167.7	62.14	6.355	34.07	14800	210.5	803
18	91.5	219.0	62.09	5.848	37.91	17170	244.5	857
19	86.5	181.2	62.14	6.138	40.47	17900	255.0	938
20	77.0	107.0	62.23	7.013	41.09	17020	242.0	1,018

* All temperatures in $^{\circ}F$.

TABLE III

"EFFECTIVE" HEAT TRANSFER COEFFICIENT, $N_{Nu}/(N_{Pr})^{\frac{1}{3}}$, AND THE STANTON NUMBER AT STATION FIVE

Test No.	G	μ $\times 10^{-2}$	N_{Re} $\times 10^{4}$	h_{fx}	η_{fx} $\times 10^{-1}$	k $\times 10^{-2}$	N_{Nu}	$(N_{Pr})^{\frac{1}{3}}$ $\times 10^{-1}$	$\frac{N_{Nu}}{(N_{Pr})^{\frac{1}{3}}}$	N_{St} $\times 10^{-2}$
1	4840	4.84	2.34	16.5	7.24	1.67	230	8.90	268	1.42
2	5926	4.84	2.87	18.5	7.08	1.69	256	8.90	288	1.30
3	6340	4.84	3.07	19.3	6.95	1.61	281	8.90	316	1.27
4	8050	4.87	3.87	21.7	6.75	1.66	306	8.90	344	1.12
5	7690	4.56	3.95	23.4	6.24	1.54	354	8.96	395	1.27
6	10950	4.99	5.13	26.9	6.40	1.73	364	8.87	411	1.025
7	11600	4.61	5.89	28.0	6.27	1.58	414	8.95	462	1.005
8	12820	4.98	6.03	29.7	6.19	1.72	417	8.87	479	0.965
9	16060	5.22	7.19	35.8	5.88	1.83	457	8.84	517	0.929
10	15200	4.78	7.44	32.5	5.93	1.61	474	8.91	531	0.893
11	16340	4.94	7.75	36.3	5.75	1.71	496	8.87	560	0.925
12	16120	4.80	7.86	36.3	5.76	1.65	515	8.85	583	0.937
13	16920	4.91	8.07	39.0	5.61	1.69	540	8.84	611	0.960
14	18410	5.18	8.32	41.6	5.51	1.81	537	8.84	608	0.941
15	17710	4.96	8.36	38.2	5.63	1.72	520	8.87	585	0.898
16	17910	4.95	8.47	42.1	5.36	1.71	576	8.87	650	0.979
17	18090	4.95	8.55	38.2	5.63	1.71	524	8.87	591	0.880
18	19300	5.27	8.56	42.0	5.55	1.84	533	8.84	604	0.906
19	21100	5.03	9.81	43.3	5.35	1.74	584	8.86	659	0.855
20	22920	4.63	11.1	46.0	5.28	1.56	690	8.96	769	0.835

TABLE IV

"EFFECTIVE" AVERAGE HEAT TRANSFER COEFFICIENT, $N_{Nu}/(N_{Pr})^{\frac{1}{3}}$ AND THE STANTON NUMBER

Test No.	Tube Wall Temp.* at Stations 4	6	L.M.T.D.	h_{fa}	$\eta_{fa} \times 10^{-1}$	N_{Nu}	$\frac{N_{Nu}}{(N_{Pr})^{\frac{1}{3}}}$	$N_{St} \times 10^{-2}$
1	308.0	349.0	186.2	16.3	7.35	228	256	1.40
2	300.0	340.0	180.5	17.1	7.19	236	265	1.20
3	288.0	330.0	169	18.5	7.08	269	302	1.22
4	290.0	323.0	165.2	19.1	7.0	270	304	0.99
5	228.0	262.3	150.0	21.6	6.76	329	367	1.17
6	307.0	346.0	160.4	19.8	6.90	268	302	0.75
7	206.0	247.0	120.1	28.1	6.37	416	465	1.01
8	263.0	288.0	112.3	31.2	6.08	425	479	1.02
9	288.5	325.2	104.0	35.0	5.80	458	518	0.97
10	216.4	354.0	111.0	32.4	5.93	470	527	0.89
11	240.0	275.3	99.3	36.7	5.77	503	568	0.94
12	220.5	256.0	102.2	35.6	5.78	504	570	0.92
13	227.8	259.6	92.0	41.2	5.49	570	655	1.01
14	275.0	310.9	91.6	41.2	5.49	533	603	0.93
15	237.0	273.0	93.7	40.8	5.41	556	626	0.96
16	235.0	264.0	90.4	41.9	5.51	585	660	0.97
17	234.0	267.2	91.7	41.4	5.49	566	639	0.95
18	285.5	319.5	88.0	43.7	5.38	557	630	0.94
19	242.5	272.0	84.3	46.5	5.26	625	705	0.92
20	166.0	195.0	81.3	49.0	5.18	737	824	0.90

* All temperatures in ^{o}F.

TABLE V

THE LOCAL AND AVERAGE HEAT TRANSFER COEFFICIENTS BASED ON HUNDRED PER CENT EFFICIENCY OF THE FINS

Test No.	h'_{fx}	N'_{Nux}	$\frac{N'_{Nu}}{(N_{Pr})^{\frac{1}{3}}}$	h'_{fa}	N'_{Nua}	$\frac{N'_{Nua}}{(N_{Pr})^{\frac{1}{3}}}$
1	12.3	171	193	12.2	171	192
2	13.4	185	209	12.6	174	196
3	13.5	196	221	13.4	195	219
4	15.3	216	243	13.7	193	217
5	15.1	229	256	15.1	229	256
6	18.1	245	276	14.2	192	217
7	18.5	274	306	18.8	278	311
8	19.1	259	292	20.2	275	310
9	22.2	283	321	22.3	285	323
10	21.1	307	344	20.5	298	334
11	22.4	306	345	22.9	314	353
12	22.7	322	364	22.2	315	356
13	23.6	327	370	24.7	342	387
14	25.0	323	365	24.8	321	363
15	24.0	326	368	24.2	329	372
16	24.5	335	378	25.1	344	377
17	23.3	319	360	24.7	346	382
18	25.5	327	370	25.8	328	371
19	25.6	329	372	27.0	363	410
20	26.8	402	449	27.9	414	461

TABLE VI

CONVECTIVE HEAT TRANSFER COEFFICIENT, CALCULATED FROM THE HEAT BALANCE ON AIR BETWEEN STATIONS FOUR AND SIX, AND BASED ON HUNDRED PER CENT EFFICIENCY OF THE FINS

Test No.	W	Δt of air between stations 4 and 6	$\Delta t \times W \times C_p$	L.M.T.D.	h	N_{Nu}	$\frac{N_{Nu}}{(N_{Pr})^{\frac{1}{3}}}$
1	215	29.2	1509	186.2	8.5	119	134
2	263	22.8	1440	180.5	8.4	117	131
3	281	23.6	1590	169.0	9.0	144	162
4	357	16.2	1390	165.2	8.8	125	171
5	342	18.3	1500	150.0	10.5	159	177
6	486	11.1	1295	160.4	8.4	114	129
7	515	10.3	1274	120.1	11.1	165	184
8	569	9.7	1323	112.3	12.4	169	190
9	713	7.0	1200	104.0	12.1	155	175
10	674	4.7	761	111.0	6.9	100	113
11	729	6.2	1084	99.3	11.5	158	178
12	716	6.8	1170	102.2	12.0	170	192
13	753	8.8	1590	92.0	18.9	259	288
14	818	6.4	1258	91.6	14.4	186	210
15	786	6.9	1302	93.8	14.5	197	223
16	795	7.6	1450	90.4	16.7	229	258
17	803	8.0	1541	91.8	17.6	241	272
18	857	5.7	1172	88.0	13.9	177	200
19	938	5.5	1239	84.3	15.4	207	234
20	1018	5.6	1367	81.3	17.6	264	294

TABLE VII

CONVECTIVE HEAT TRANSFER COEFFICIENT AND $N_{Nu}/(N_{Pr})^{\frac{1}{3}}$ BASED ON A NEW EQUIVALENT DIAMETER d_e

Test No.	G	N_{Re} $\times 10^4$	$\Delta t \times W \times C_p$	L.M.T.D.	h'_{fa}	N_{Nu}	$\frac{N_{Nu}}{(N_{Pr})^{\frac{1}{3}}}$
1	4840	1.42	1509	186.2	8.5	69	78
2	5926	1.75	1440	180.5	8.4	71	80
3	6340	1.87	1590	169.0	9.9	87	98
4	8050	2.36	1390	165.0	8.8	76	86
5	7690	2.41	1500	150.0	10.5	97	108
6	10950	3.14	1295	160.4	8.5	71	80
7	11600	3.59	1274	120.1	11.1	96	107
8	12820	3.68	1323	112.3	12.3	98	111
9	16060	4.39	1200	104.0	12.1	94	106
10	15200	4.55	761	111.0	7.2	64	72
11	16340	4.73	1084	99.3	11.4	96	108
12	16120	4.80	1170	102.2	12.0	104	118
13	16920	4.82	1590	92.0	18.1	153	173
14	18410	5.09	1258	91.6	14.4	114	129
15	17710	5.11	1302	93.8	14.6	121	137
16	17910	5.18	1450	90.4	16.8	141	159
17	18090	5.21	1541	91.8	17.6	147	166
18	19300	5.23	1172	88.0	14.0	108	122
19	21100	6.00	1239	84.3	15.4	126	142
20	22920	7.07	1367	81.3	17.6	161	179

TABLE VIII

RADIAL FIN TEMPERATURE GRADIENT AT STATION FIVE

Test No.	Fin temperatures*					Average air temp. at station 5
	From thermocouples			Calculated		
	at x = 3/16"	at x = 1/2"	at x=L=1"	at x = 3/16"	at x = 1/2"	
1	236.3	253.5	326.9	235.5	267.6	141.1
2	218.9	234.5	307.1	218.8	248.3	138.1
3	219.4	235.0	305.1	218.6	247.5	141.2
4	203.5	219.2	287.9	209.7	220.8	139.9
5	163.5	178.6	249.0	163.8	191.9	99.5
6	214.0	225.0	292.0	217.0	240.3	171.9
7	151.6	164.3	228.7	150.4	174.8	106.0
8	207.0	220.8	279.9	204.2	228.2	163.0
9	239.9	253.7	306.6	259.1	263.9	213.5
10	163.8	177.3	236.3	165.6	189.3	128.5
11	190.5	202.0	260.5	208.7	209.9	159.1
12	169.3	182.1	240.3	168.4	189.7	138.8
13	182.9	194.5	248.0	178.6	197.8	152.4
14	230 3	241.3	292.0	225.6	245.8	201.0
15	192.0	203.2	257.2	186.9	205.5	159.7
16	187.9	198.5	252.8	183.3	203.4	160.0
17	188.1	198.7	254.2	183.9	201.2	156.8
18	238.6	249.3	302.6	230.5	251.2	206.0
19	202.5	214.5	261.0	194.2	212.9	172.1
20	123.0	132.0	184.3	119.4	137.1	99.6

* All temperatures in ^{o}F.

Figure 16. Heat Transfer Curve at Station Five.

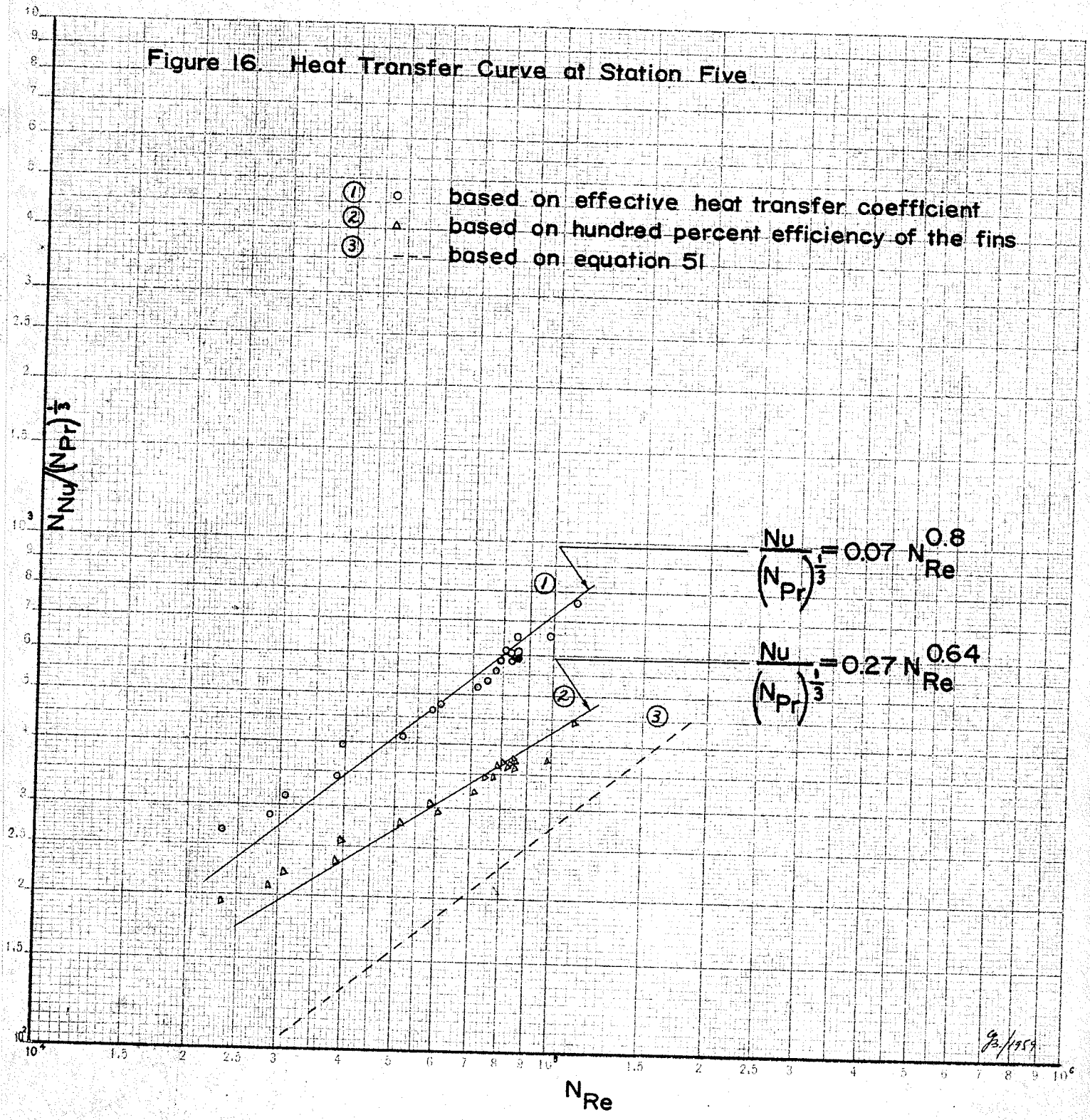

Figure 17. Heat Transfer Curve Between Stations Four and Six.

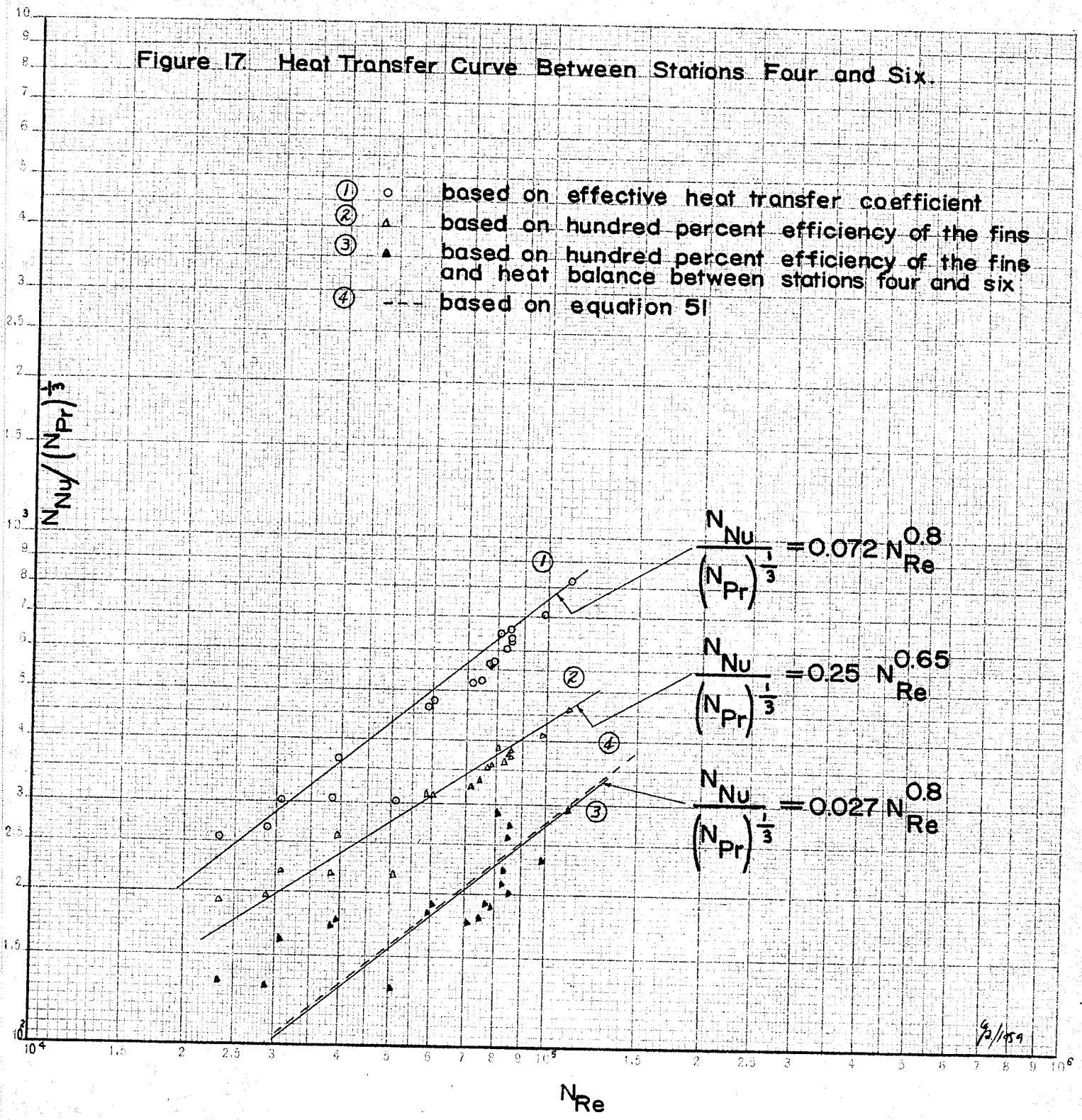

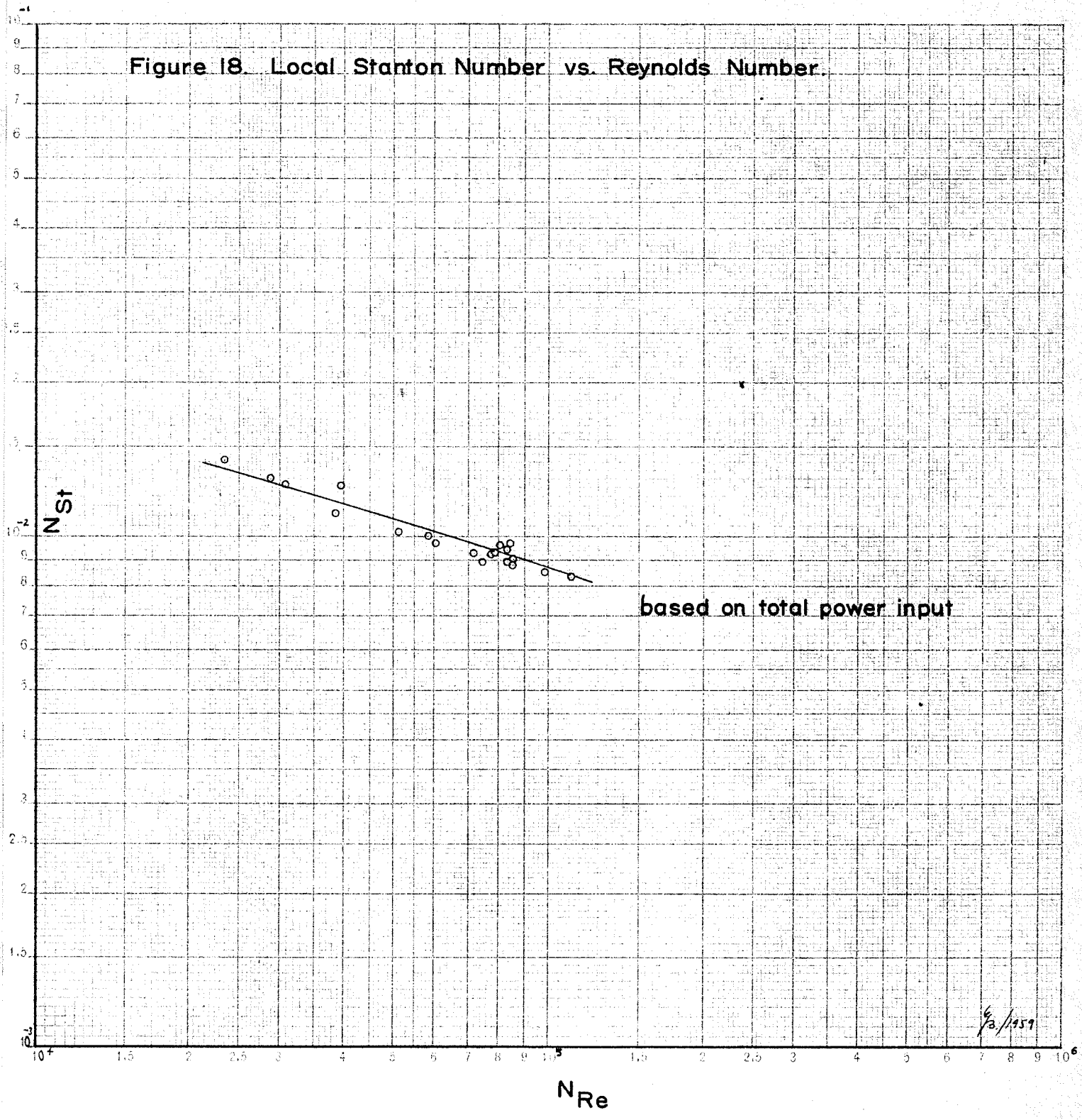

Figure 18. Local Stanton Number vs. Reynolds Number.

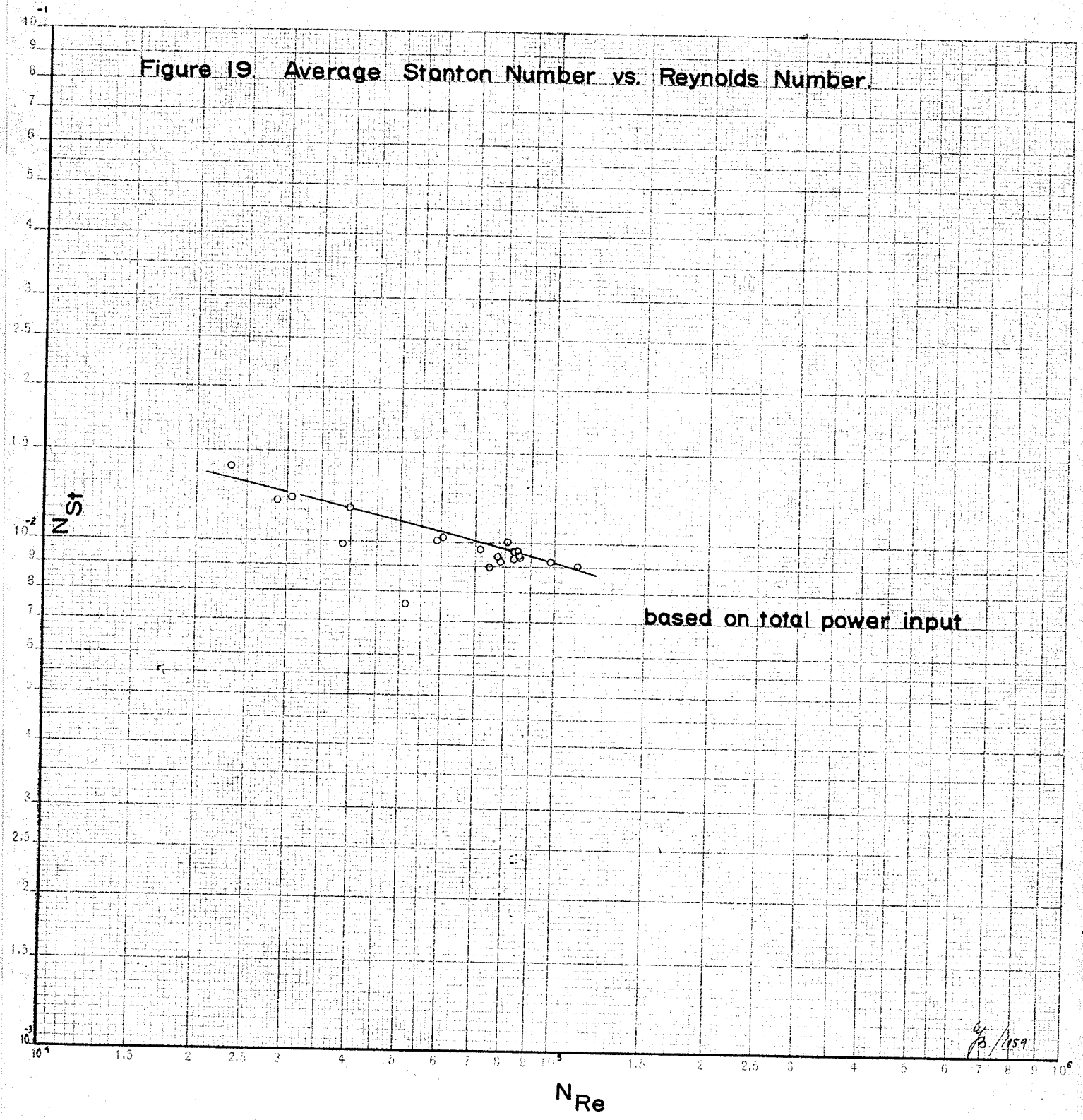

Figure 19. Average Stanton Number vs. Reynolds Number.

Figure 20. Heat Transfer Curve Between Stations Four and Six, Based on the New Equivalent Diameter d_e.

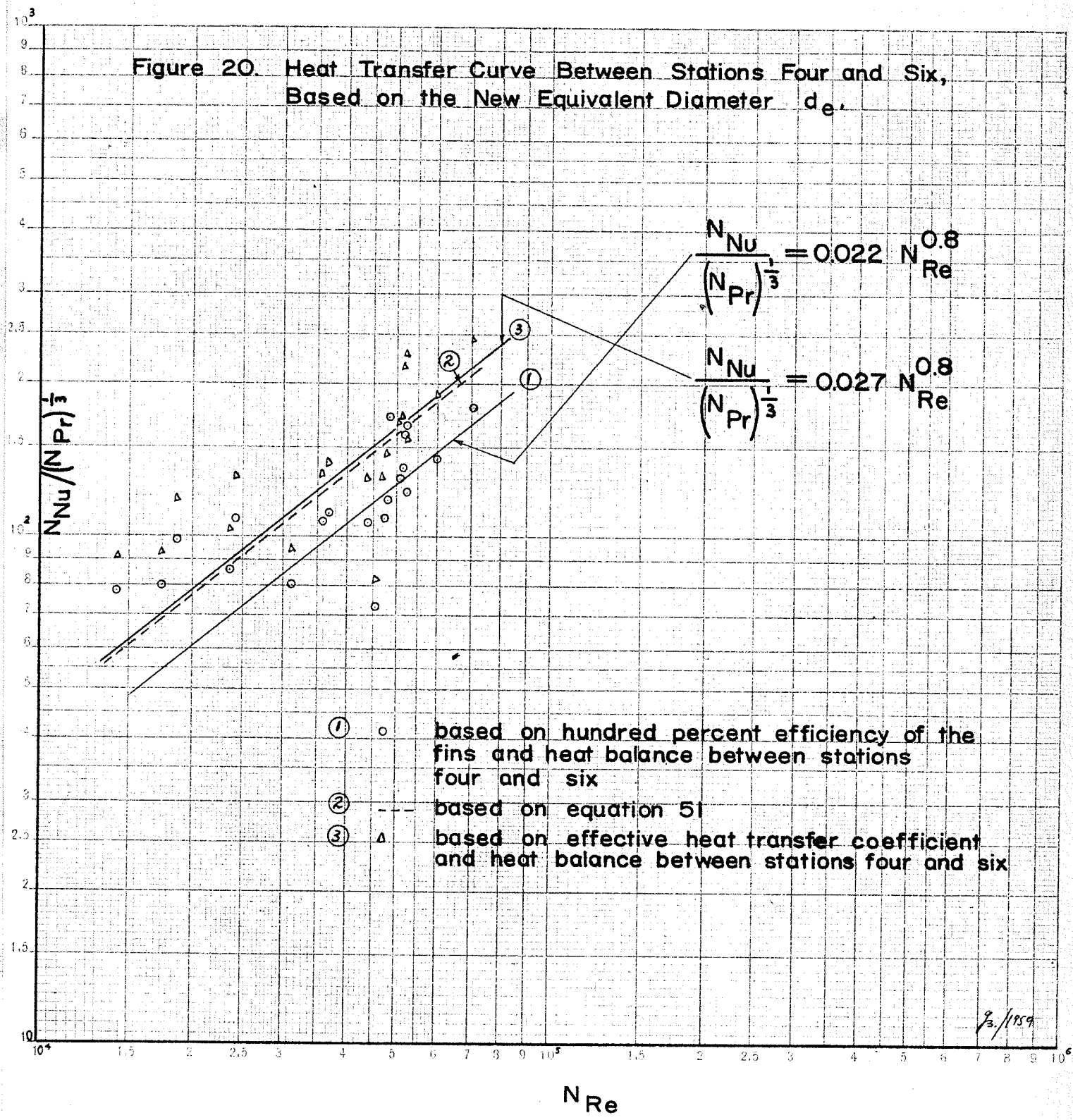

Figure 21. Heat Transfer Curve Based on Heat Balance Between Stations Four and Six and D_e.